ORNL/TM-7452

ornl

OAK
RIDGE
NATIONAL
LABORATORY

UNION
CARBIDE

ISX-B Neutral Beams and the Beam Target Experiment

S. C. Bates
P. H. Edmonds
J. Kim
C. E. Bush
L. A. Massengill
D. R. Overbey
J. W. Pearce

OPERATED BY
UNION CARBIDE CORPORATION
FOR THE UNITED STATES
DEPARTMENT OF ENERGY

DISCLAIMER

Printed in the United States of America. Available from
National Technical Information Service
U.S. Department of Commerce
5285 Port Royal Road, Springfield, Virginia 22161
NTIS price codes—Printed Copy: A04; Microfiche A01

ORNL/TM-7452
Dist. Category UC-20 f

Contract No. W-7405-eng-26

FUSION ENERGY DIVISION

ISX-B NEUTRAL BEAMS AND THE BEAM TARGET EXPERIMENT

S. C. Bates, P. H. Edmonds, J. Kim, C. E. Bush,
L. A. Massengill, D. R. Overbey, and J. W. Pearce

Date Published - October 1980

Prepared by the
OAK RIDGE NATIONAL LABORATORY
Oak Ridge, Tennessee 37830
operated by
UNION CARBIDE CORPORATION
for the
DEPARTMENT OF ENERGY

THIS PAGE

WAS INTENTIONALLY

LEFT BLANK

CONTENTS

THIS PAGE

WAS INTENTIONALLY

LEFT BLANK

ABSTRACT

This report describes the hardware and operation of the ISX neutral beamlines as well as an experiment done to verify estimates of the neutral power injected into the tokamak.

Tangential coinjection of megawatt levels of 30-40-keV neutrals into the tokamak has made the study of high-beta plasmas in ISX possible. These power levels were achieved with high reliability (over 90%) by two neutral beamlines with design power ratings of 900 kW of H^0 (upgraded to 1.5 MW) each. The neutral beamlines consist of a duoPIGatron plasma generator, acceleration grids, a gas neutralization cell, an ion deflection magnet, beam calorimetry, high-speed helium cryocondensation vacuum pumps, and associated electrical and control systems. The beamlines and their operation are described briefly with an emphasis on their relation to injection into a plasma. Neutral injection geometry with respect to the tokamak is given.

Injected power was estimated by comparison with power measured by a calorimeter in the beamline that could be inserted directly into the beam path. It was assumed that 85% of the power deposited on this calorimeter during conditioning beam pulses was injected into ISX. In July 1979 a calorimeter target was placed in the tokamak to check this estimate. Complete analysis of the data supports a 15% beam loss. Roughly half of this arises from beam particles reionized and deflected by the tokamak magnetic fields; the remaining part is due to a drop in beam voltage and current (relative to a conditioning shot) because the tokamak power supplies cause a drop in the main ac line voltage. The background gas that results in beam reionization appears to be the result of normal beamline gas flows.

The neutral beam upgrade is also briefly described.

1. INTRODUCTION

The purpose of this report is twofold. The first goal is to provide a general description of the ISX beamlines and their operation. The second is to describe an experiment that was performed on one beamline to validate injected power estimates.

One of the primary goals of ISX-B is to study the high-beta plasmas that result from large amounts of auxiliary heating. On ISX this heating is done by the injection of high-energy hydrogen neutrals tangential to the plasma axis in the same direction as the plasma ion current. These neutrals are generated by a complex system known as a neutral beamline.

There are two neutral beamlines on ISX-B with 22-cm-diam sources. As of November 1979 they had together supplied up to 1 MW of 40-keV neutrals to the plasma in 100-ms pulses.

The neutral beam atoms originate in a 22-cm-diam plasma source of a special type, called a duoPIGatron plasma generator. From this plasma, ions are extracted and accelerated by a set of three grids (one prevents electron backstreaming). A majority of the ions are then converted to neutrals in a gas cell. Any ions still remaining in the beam are removed as they pass between the poles of a bending magnet. Finally the high-energy neutrals pass through a transition section and into the tokamak.

The injection of a neutral beam into an ISX-B discharge is only a small part of the overall task of neutral injection. Each beamline is an independent and complex system. Its major components are the beam calorimetry, the cryopump and vacuum system, and the ion source. The ion source is the most critical component; it must be operated frequently to achieve and maintain given operating parameters in what is known as a conditioning process. Beamline performance is rated primarily in terms of the neutral power that is available for injection.

The neutral beam power that is injected cannot be measured directly, but it can be inferred in various ways. The primary diagnostic for beam power is a water-cooled calorimeter that is inserted into the beam path during conditioning shots and retracted for injection. The actual

injected power is determined by duplicating beam parameters as closely as possible, comparing conditioning and injection shots. Injection power is estimated using measured conditioning power and known losses during injection.

To check the validity of this estimation a set of experiments was done with a calorimetric target that was placed inside the tokamak to intercept one beam. The power on this target was compared with that measured by the calorimeter in the beamline for varying beam conditions and toroidal fields. Additional instrumentation on the target and tokamak made beam profile and beam time-history studies possible.

2. ISX-B NEUTRAL BEAMS — DESCRIPTION

2.1 INTRODUCTION

The ISX-B neutral beamlines are for the most part copies of the beamline developed by the Plasma Technology Section at Oak Ridge National Laboratory (ORNL) for use on the Princeton Large Torus (PLT). This work has yielded much information on beamline performance and characteristics.[1,2] In particular, experiments have been done with ion sources similar to those used on ISX, i.e., on a beamline simulating the tokamak injection geometry.[3]

Since the beamlines are described in detail elsewhere, the description here will be mostly superficial except where differences exist. Emphasis is placed on the beamline operating environment.

2.2 ISX BEAMLINES — HARDWARE

A schematic drawing of an ISX beamline is shown in Fig. 1. The ion source generates a 22-cm-diam hydrogen ion beam. The ion beam is neutralized in a gas cell, and the remaining ions are diverted to a particle dump by a deflection magnet. The low pressures required for tokamak plasmas are maintained during the beam pulse by high-speed (≈200,000-liter/s) cryocondensation pumps that saddle the gas cell. These pumps consist of stainless steel panels cooled to liquid helium temperatures (≅4°K).

At the end of the beamline tank, any stray beam particles are scraped off by a set of four adjustable beam-defining plates (a rectangular opening). This minimizes the beam loading on the walls of the drift duct leading to the tokamak. Almost all of the beam that emerges from the defining-plate aperture (e.g., 18 × 18 cm) is injected into the tokamak (this ignores losses from background gas). Beam power is measured by a water-cooled calorimeter in the drift duct downstream of the defining aperture; the calorimeter retracts during an injection shot. The beamline is electrically isolated from the tokamak and can be vacuum isolated by a valve at the end of the beamline.

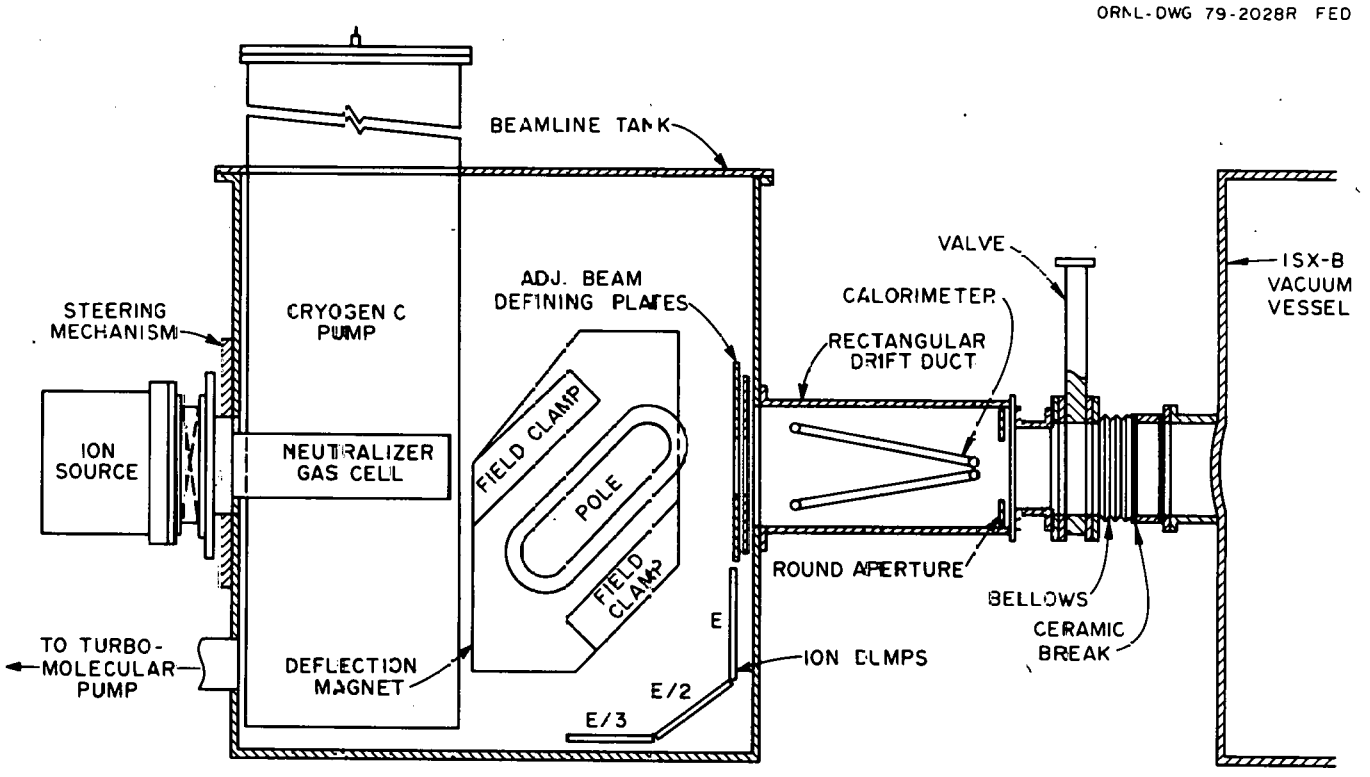

Fig. 1. ISX-B neutral beamline schematic.

The most critical part of a beamline is the ion source. The basic ISX-B sources use 22-cm-diam duoPIGatron plasma generators with a shaped-aperture acceleration grid. The source and accelerator geometry are shown in Fig. 2. Detailed operation of the source is described elsewhere.[4,5] Basic parameters of operation include arc current and voltage, cathode and anode chamber gas flow rates, source magnet strength, and acceleration voltage. Deceleration potential is variable but has little effect beyond a minimum value. There are 1799 apertures in the grids, giving a 37% transparency; all of the grids are water cooled.

The injected beams have a design power of 900 kW for 100 ms. This power is about 35% of the accel supply power that is extracted from the grids as 61 A of 42-kV ions, representing maximum beam performance. Figure 3 shows the power accountability along the simulated ISX beamline of the Plasma Technology Section. No power accountability was attempted on the ISX beamlines; only the beam-dump calorimeter and the beam-defining plates were monitored. Figure 4 shows the ISX source performances as a function of extracted current at constant voltage.

The beam, made up of many beamlets, is focused at a point 4.0 m from the grids to permit maximum transmission through the beam port on the tokamak. The neutralization efficiency of the gas cell is about 60%; the beam species yield is 80% H_1^0 (E), 12% H_1^0 (E/2), 7% H_1^0 (E/3), $+H_2^0$, where E is the acceleration energy (40 kV nominal).[6]

There are three independent sets of instruments for each beamline: one for the beamline vacuum and water-cooling systems, one for the cryopumps, and one for the sources and power supplies. Crucial to injection documentation are the beam current and voltage monitors and the drift duct calorimeter power monitor. The former were accurate but sometimes failed entirely; the latter was subject to significant error.

The power monitor converts the flow rate and temperature rise of the cooling water into a digital display of deposited energy for the drift duct calorimeter and the defining plates. In operation it required constant attention to keep thermal drift errors minimal.

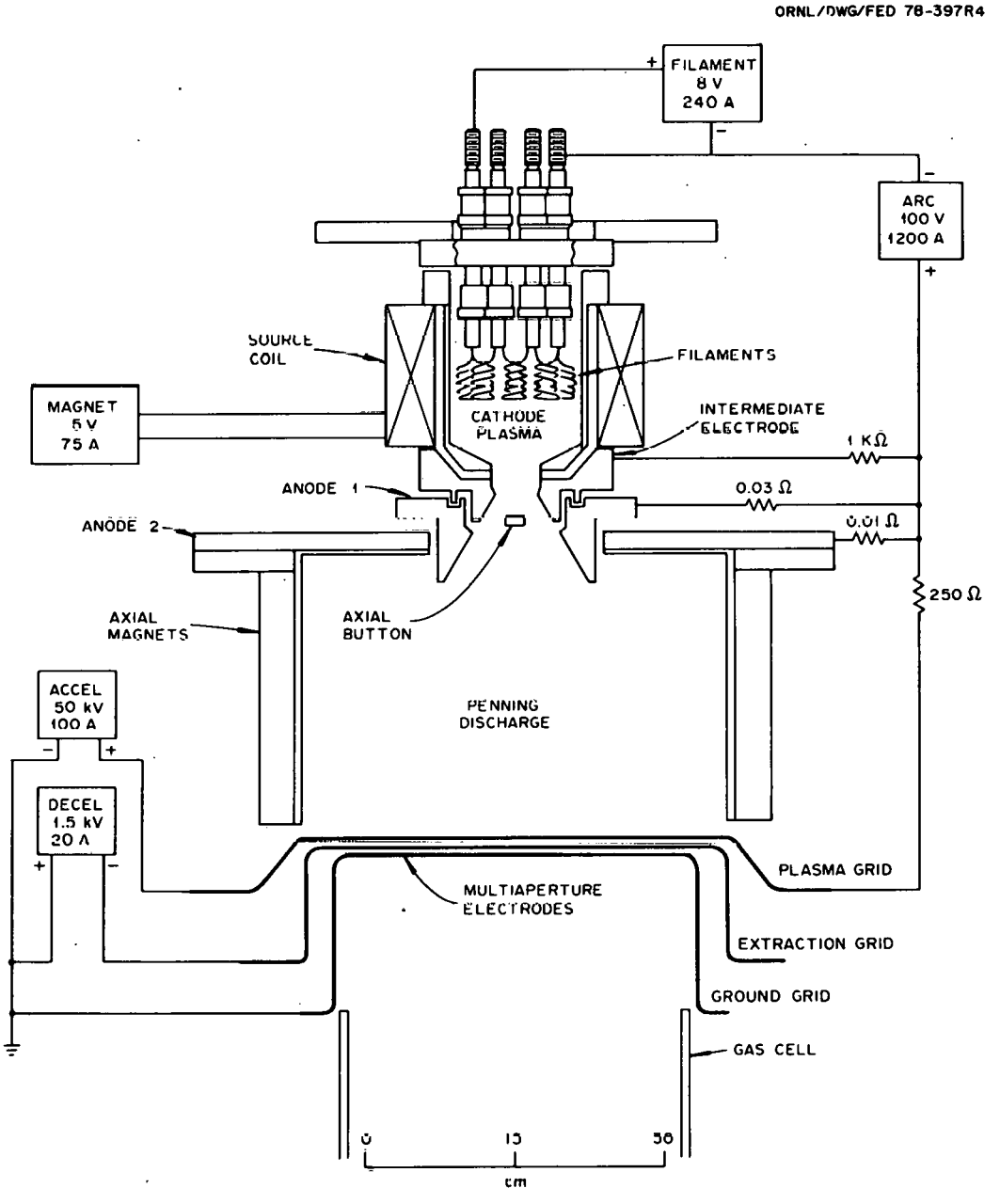

Fig. 2. DuoPIGatron plasma source with extraction grids.

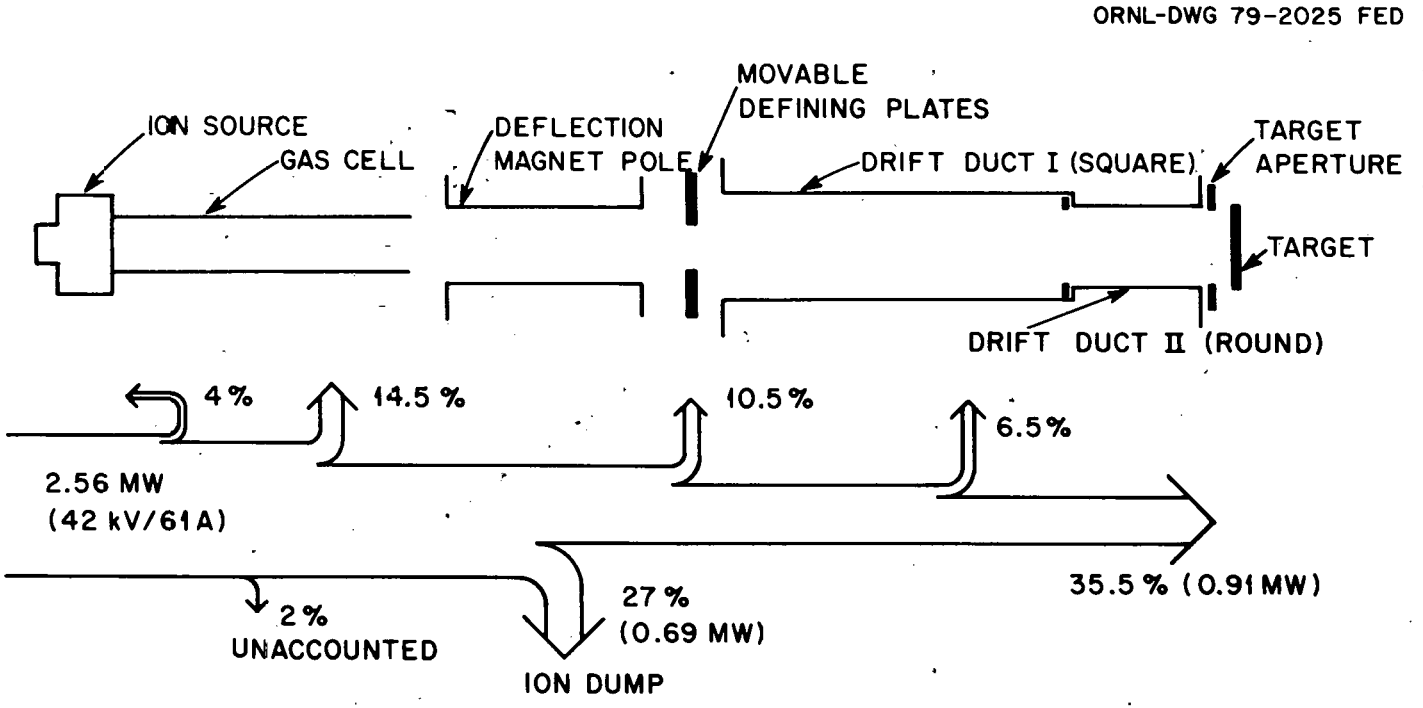

Fig. 3. Beamline extracted power flow schematic.

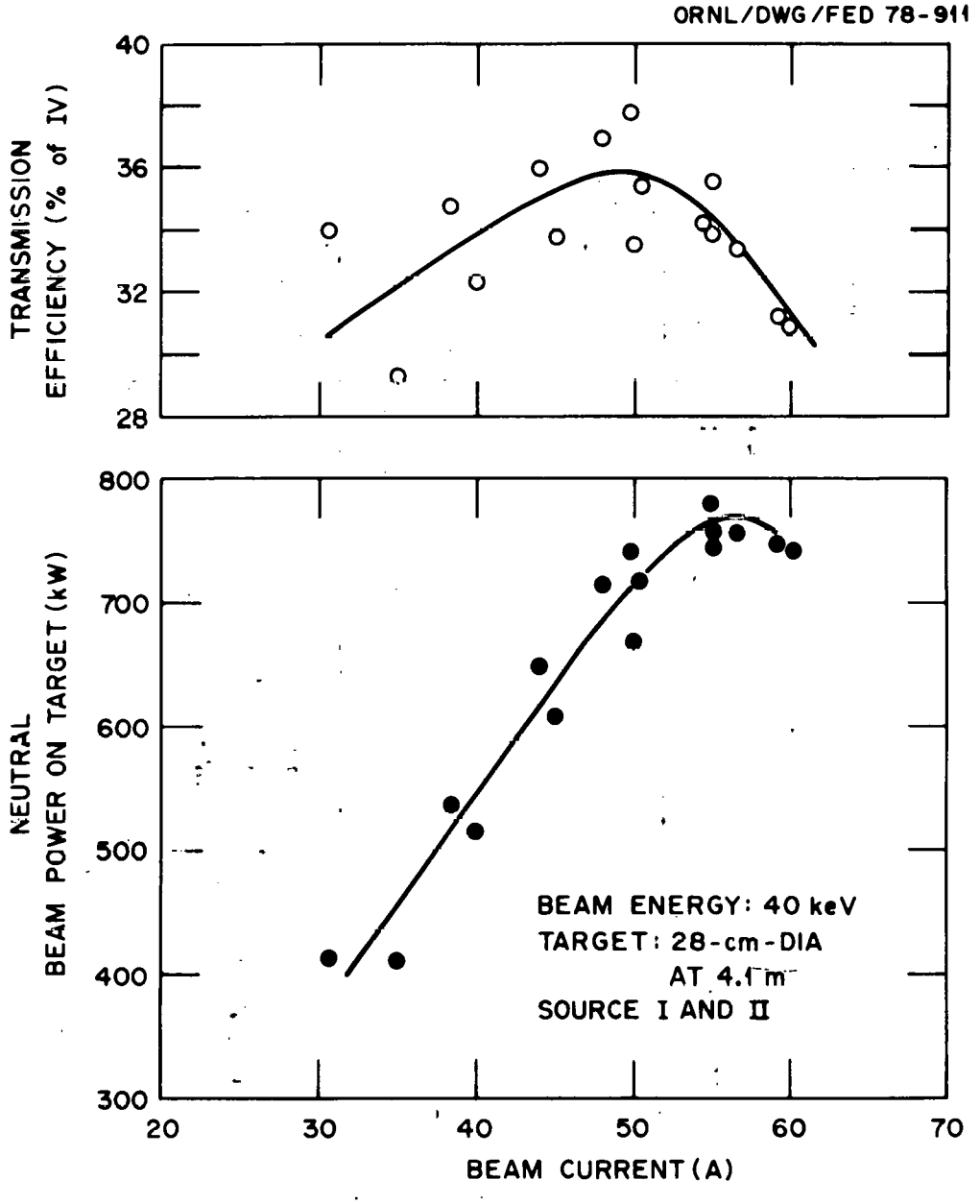

Fig. 4. ISX 22-cm source performance curves.

2.3 ISX INJECTION GEOMETRY

The geometry of neutral injection into ISX is shown in Fig. 5 (before the upgrade). The beamlines, known as East and West, inject into sectors 16 (West) and 1 (East), 60° apart. The measurements are given with respect to the vacuum vessel; actual beam deposition in the plasma is a combination of the beam and plasma properties on each particular shot. The beams are aimed well inside the plasma centerline to maximize the path length of the beam particles through the plasma. The nominal beam focus is at 4.0 m, but this value can vary slightly as the grid shape and spacing vary during the lifetime of the source.

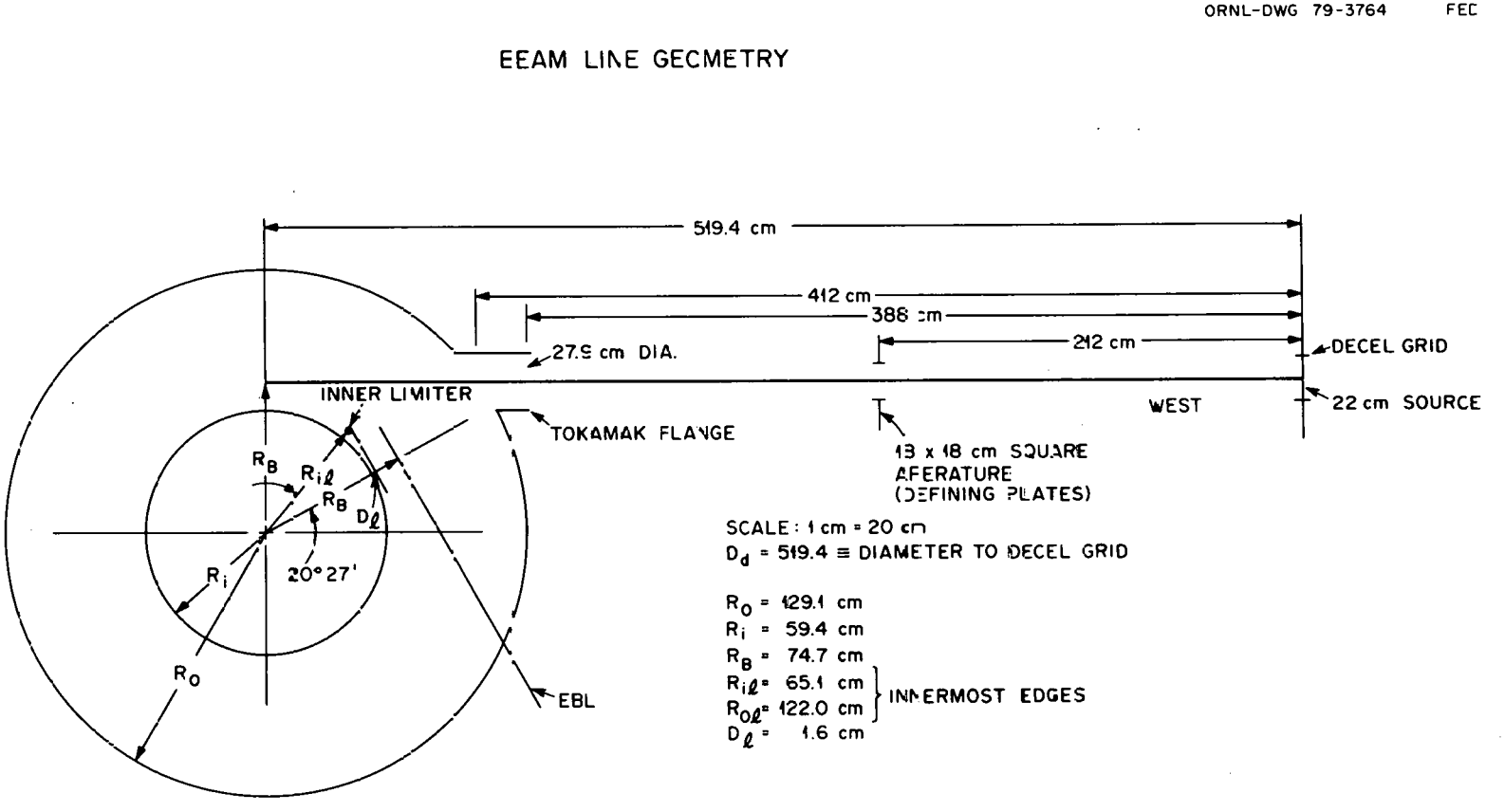

Fig. 5. ISX neutral injection geometry.

3. BEAMLINE OPERATION

There are two primary phases of ISX beamline operation: conditioning and injection. The neutral beams are a tool for the operation of the tokamak so that injection takes precedence over all other phases of beamline operation. Conditioning or other beamline work is an ongoing process to improve injection performance or increase injection power.

3.1 THE NEUTRAL INJECTION PROCESS

The most common starting conditions for injection are for the beamlines to be opened to the tokamak vacuum while the drift duct calorimeter is closed and the sources are being conditioned with pulses every 5-10 s. At 5-30 s before a shot the calorimeter is opened, leaving a clear path to the tokamak and enabling the injection interlock. This interlock causes the source-sequencing timer to wait until an initialization pulse arrives from the tokamak control room 1 s before the beam firing time t_b, assuming that related interlocks indicate proper operation of all systems. When the pulse arrives, the sequencer begins a source cycle. At 100-200 ms before t_b, the source and gas cell gas feeds turn on. At about 5 ms before t_b, accel(erator) and decel-(erator) voltages are applied to the source grids. At t_b, the arc voltage is applied. This voltage initiates the source plasma, from which a beam is immediately extracted, neutralized, and injected. At t_b + 100 ms (nominally) the accel voltage is turned off and the beam pulse ends. The arc and gas feeds are turned off shortly afterward. The beam sequencing is interlocked with the plasma current so that injection only occurs in the presence of a plasma (preventing damage to the far wall of the tokamak).

Normally the beams are on for 100 ms during a 150-200-ms plasma shot. Although the timing of a beam pulse within a shot is controlled by the tokamak operator, each pulse can only occur as a result of detailed sequencing within the beamline.

The beam parameters relevant to the plasma are: power injected, pulse length, particle energy, species (H, H_2, ...), and beam cross-section profile. Only the pulse length and fundamental particle energy (accel voltage) are known accurately. Species yield and beam profile are inferred from test stand measurements, together with supportive diagnostics, and the power is inferred from beam-conditioning pulses. Injection power estimation will be discussed later.

A typical tokamak shot time history with injection is shown in Fig. 6. The most important beam parameters for neutral injection into plasma are the ion beam current and acceleration potential. These parameters define a flux and energy distribution of neutral particles injected into the tokamak. The level of beam current that can be extracted from the plasma source is in turn dependent on the arc current and arc drive voltage (typically 400-700 A, 100-130 V) and on the plasma density arising from the gas injected into the source. The injected power plot in Fig. 6 shows the beam injection in relation to a typical plasma shot. The ion temperature rises from the heating, and the plasma pressure (and consequently the beta for a fixed toroidal field) also increases.

3.2 OPERATING REALITIES

Nominally the only cause of beam performance degradation is the lifetime of the filaments that supply ionizing electrons to the source plasma. However, the sources must be continually conditioned to prevent internal arcing (high and low voltage). Repeated arcing causes irreversible damage to the source. It is likely that the sources must be cleaned periodically, but there has not been enough long-term operation to determine a cleaning schedule.

The cryopumping system is a major factor in beam operation, both in cost and schedule. The liquid helium panels that pump the excess hydrogen in the beamline are loaded up continuously during operation, and they must be warmed up (regenerated) periodically. This is usually done each weekend and is followed by cooling down to liquid helium

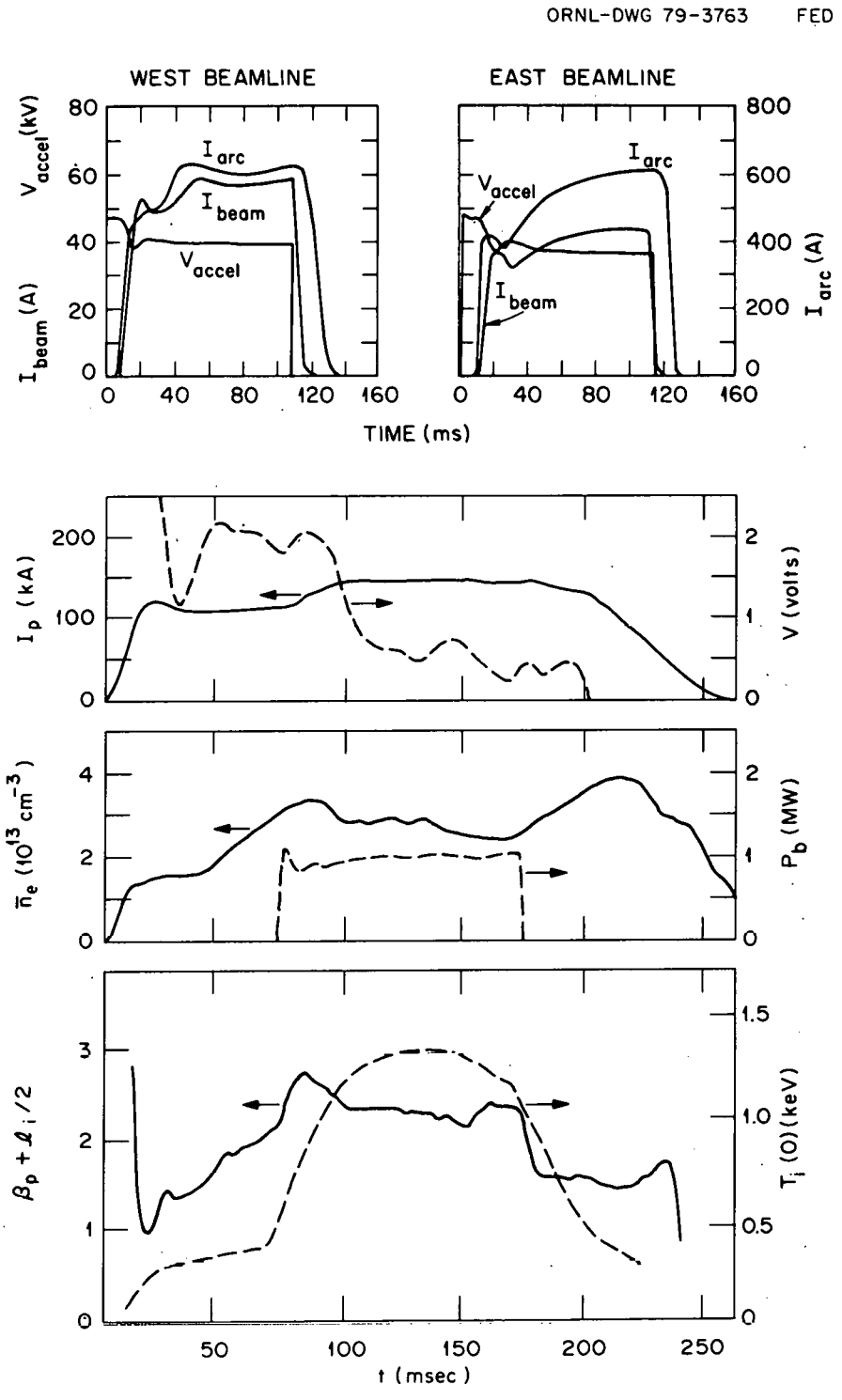

Fig. 6. Time history of ≈1 MW of two-beam neutral injection into an ISX-B plasma.

temperatures again on Monday. Cryogen consumption depends on the gas loading rate coming from conditioning or small leaks in the beamline.

Neutral beam operation also affects tokamak plasmas by changing the tokamak pressure between shots and thus altering wall conditions. Conditioning shots in the beamlines during an injection run cause significant pressure bursts in the tokamak, in spite of the cryopumps. The high pumping speed of the cryopumps results in significant pumping of the torus between pulses; the pumping is conductance limited and thus increases when the beamline calorimeter is opened. Usually the sources are conditioned between injection shots, but at somewhat reduced power levels this conditioning has been eliminated.

The neutral beam systems undergo continual repair and improvement in an attempt to reach maximum rated injection power. As of November 1979, the two beamlines have supplied up to slightly over 1 MW of injected power, compared with a nominal maximum of 1.8 MW. Operating time has been a tradeoff between available power levels and the time needed to reach higher levels.

3.3 HISTORY OF INJECTION EXPERIMENTS

Neutral injection experiments were begun in October 1978 with one beamline at a level of approximately 300 kW. Since that time injection power has increased to 1 MW; it is limited primarily by the unavailability of dedicated high-voltage power supplies. The injection history up to the November 1979 shutdown is shown in Fig. 7.

Beamline performance during injection has been studied to determine the actual reliability of this form of auxiliary heating. The results, shown in Table 1, are encouraging, indicating a 90-95% success rate. However, there is no question that the beamlines constitute a major system that approaches the tokamak in complexity and in impact on overall fusion program operation.

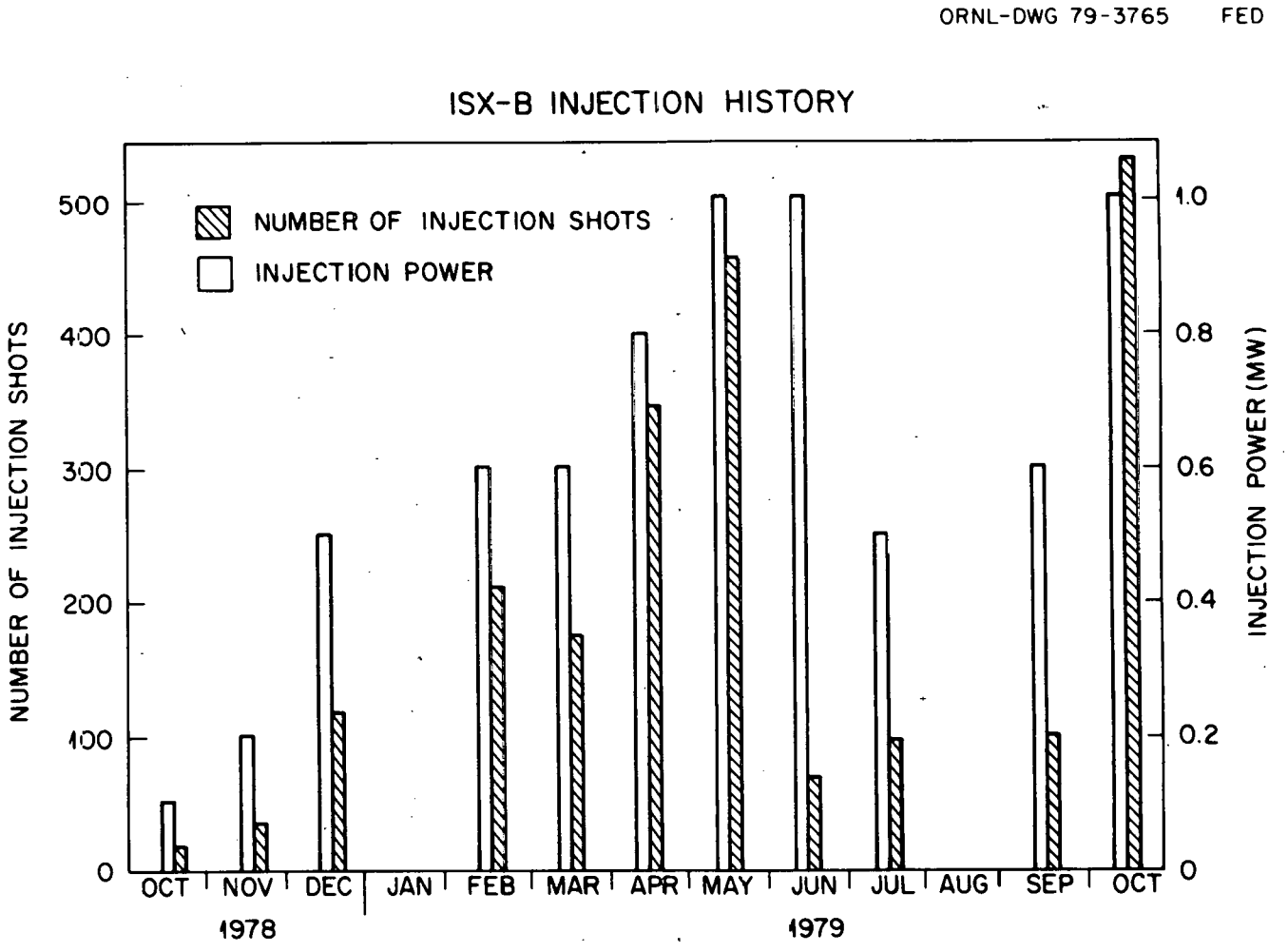

Fig. 7. Beamline operating performance for ISX-B neutral injection experiments.

Table 1. Injection reliability

Once begun injection is over 90% successful:

10/79	Failures/successes		
	10/1	1/24	
	10/2	7/102	
	10/9	0/19	
	10/11	2/48	
	10/17	4/54	2 beams
	10/18	1/40	
	10/19	4/19	
	10/25	2/106	2 beams

Average success rate: 95%

On 10/17, ≈30 tokamak injection shots (repetition rate 3-10 min) were fired without beam conditioning between shots — one failure (breakdown)

Maximum number of successes: 91 shots with both beams over a 7-h continuous period

Once injection experiments were begun, for the months of March, April, May, and October:

30 operating days

- 22 ended without problems
- 3 ended due to beam failures
- 3 ended due to tokamak failures
- 2 ended due to beam-tokamak interaction failure

4. BEAM TARGET EXPERIMENT

4.1 INTRODUCTION

On July 5-9, 1979, during the latter part of an ISX shutdown for modification, neutral beam experiments were done to verify estimates of the power injected into the plasma. An instrumented stainless steel beam target was inserted into the tokamak, and beam properties seen by the plasma were measured using the West beamline. In the 3-1/2 operating days, there were 95 tokamak shots in which the neutral beam was fired onto the target and data were taken. In addition, many conditioning beam pulses were fired onto the beamline calorimeter and some onto the target for diagnostic calibration.

4.2 EXPERIMENTAL SETUP

4.2.1 Overall Configuration

The Beam Target Experiment was performed using the West beamline. This beamline was used to take advantage of large ports on the tokamak directly above and below the beam path. The geometry and dimensions of the apparatus are shown in Fig. 8. The only equipment added to the beamline was the target and its instrumentation; the misalignment of the beam centerline with the beamline, tokamak port, and target was insignificant.

4.2.2 The Target

The beam target consisted of two stainless steel plates 43 × 13.3 × 2.5 cm thick. The plates were water cooled by copper tubing brazed to the back of the plates. The plates were supported separately by 1.6-cm-diam tubes from a flange in the bottom of the tokamak. Embedded halfway between the front and rear surfaces of the target plates was a vertical and horizontal crossed array of chromel-alumel thermocouples. The geometry of the water lines and thermocouples is shown in Fig. 9.

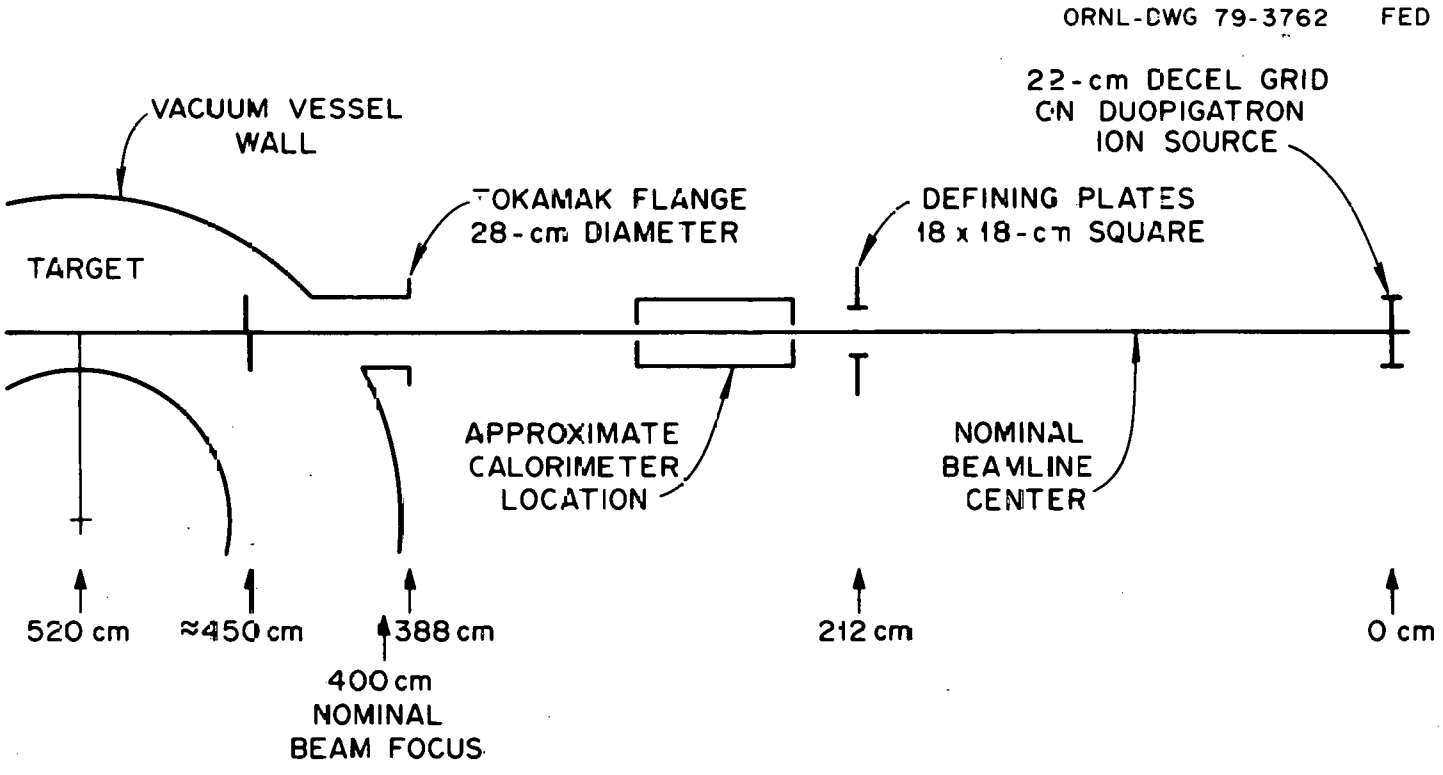

Fig. 8. Beam target experiment geometry.

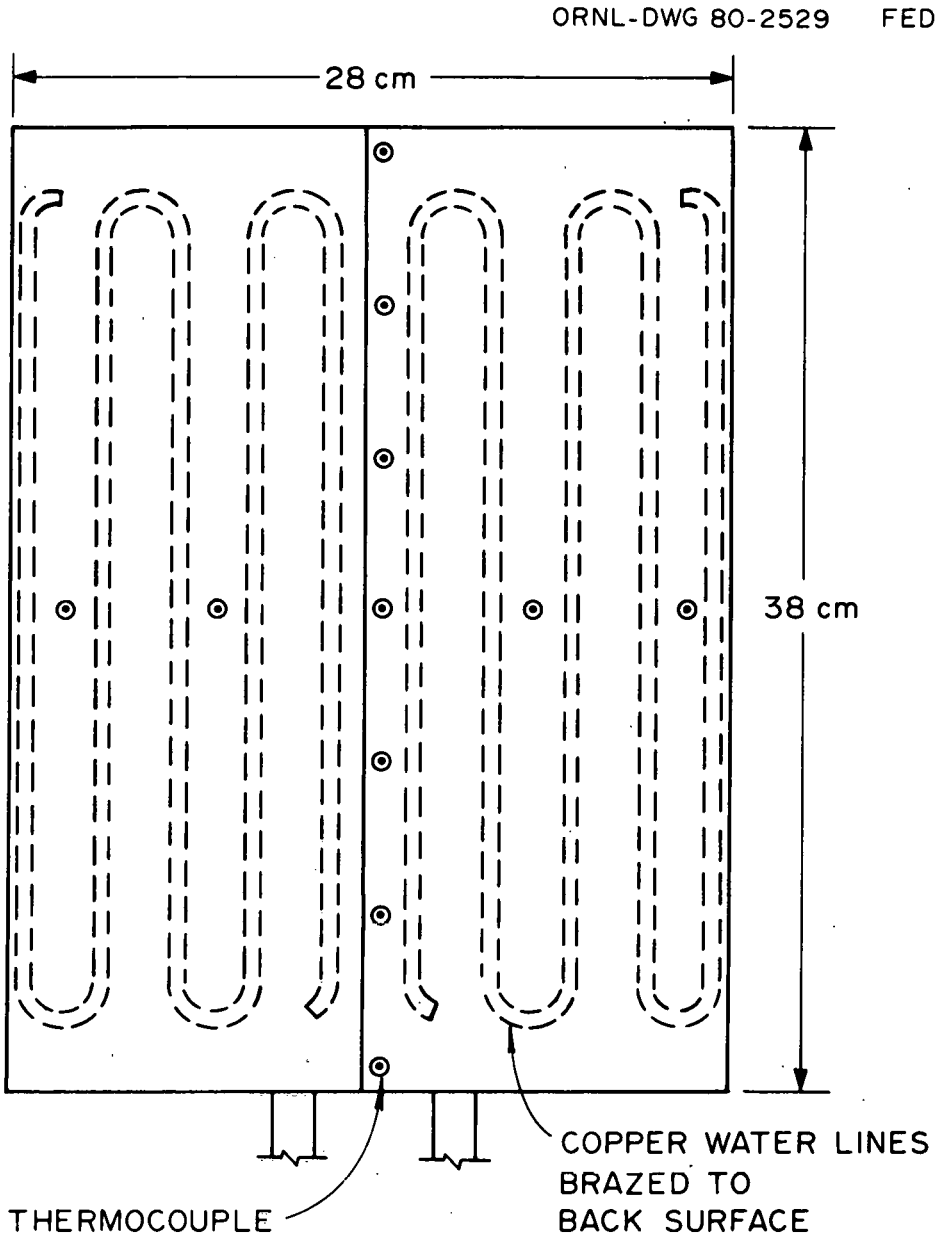

Fig. 9. Geometry of the stainless steel, water-cooled target.

The target plates could be separately rotated or moved vertically and then locked. The support flange on the tokamak was made so that when the plates were rotated to be normal to the beam, the center of the beam would fall on the center thermocouple. Thus the target was properly positioned by first adjusting the height of the support tubes to a predetermined value. Next, a straightedge was placed on the window above the target and aligned to be parallel with the beamline isolation gate valve. The target was then made normal to the beam by aligning its front surfaces with the straightedge. Experimental results without exception confirmed the accuracy of this procedure.

4.2.3 Diagnostics and Other Equipment

The primary diagnostics used for the experiment are the power monitors on the beamline and on the target, and the standard source parameter diagnostics (beam voltage, current, arc voltage, and current, etc.). The power monitor on the target sums the power on the two halves, giving a digital energy readout ($S \times \Delta T \partial t$, where S is the flow rate) as done for the beamline calorimeter. The basic comparison is between the target power monitor and the drift duct calorimeter power monitor.

The thermal response of the target to beam power deposition is measured by the thermocouple array embedded in the plates. At the location of the thermocouples (0.3 cm deep) the characteristic time for beam heating of the target is 5-10 s, so that the slow time response of the thermocouples themselves ($\approx$1 s) is an adequate measure of the deposited power. Furthermore, since the thermal time constant is so low and gradients through the plates are much higher than those across the plates, lateral thermal diffusion is negligible. Thus the thermocouple array measures the relative spatial distribution and magnitude of the 0.1-s beam pulse in its tens-of-seconds time history. Computer programs more accurately simulate this process. Each thermocouple is sampled every 2 s by a computer data acquisition system and the time history is stored for each shot.

The target surface thermal time response is measured with a commercially available infrared (IR) camera. The camera's output takes two

forms: photographic temperature profiles of the surface at different times after the beam pulse, and line scans across the target of the surface temperature during and after the beam pulse. The camera looks through a window in the tokamak so it can view the entire target.

The beam profile is measured in one form by the target thermocouple array, and in another form by an array of eight photodiode tubes that look down from a window above the target and record the light emitted from the beam as it passes through the background gas. The photodiode tubes collimate light from the beam and are pointed so that the array gives a line-integral profile of the beam as an output (Fig. 10). The output signal actually measures the product of beam particle density and background pressure, but the beam profiles derived in this way can be compared with those derived from the target thermocouples.

The tokamak gas puff system was used to provide the background pressure for the photodiode diagnostic, and the tokamak toroidal field was fired to study the effect of gas evolution with consequent beam losses due to reionization of part of the neutral beam and deflection by the magnetic field.[7]

The tokamak computers were used to record the photodiode and thermocouple data as well as to fire "shots" with and without the toroidal field. Each shot gave one data set on the beam and target.

4.3 EXPERIMENTAL PROCEDURE

The Beam Target Experiment was conducted primarily in the tokamak shot format. A tokamak operator triggered the beam pulse onto the target in addition to the data acquisition computers, the toroidal field, and the gas puff when they were used. A beam operator set the injection parameters to the appropriate values during beam-conditioning pulses between shots.

Photodiode, thermocouple, toroidal field, and gas puff data recording was automatic during each shot. Beam parameters were recorded photographically from oscilloscope traces of each shot. Power monitor outputs were recorded manually in a logbook of the experiment, together with other notes relevant to the experiments. The IR camera data were taken independently.

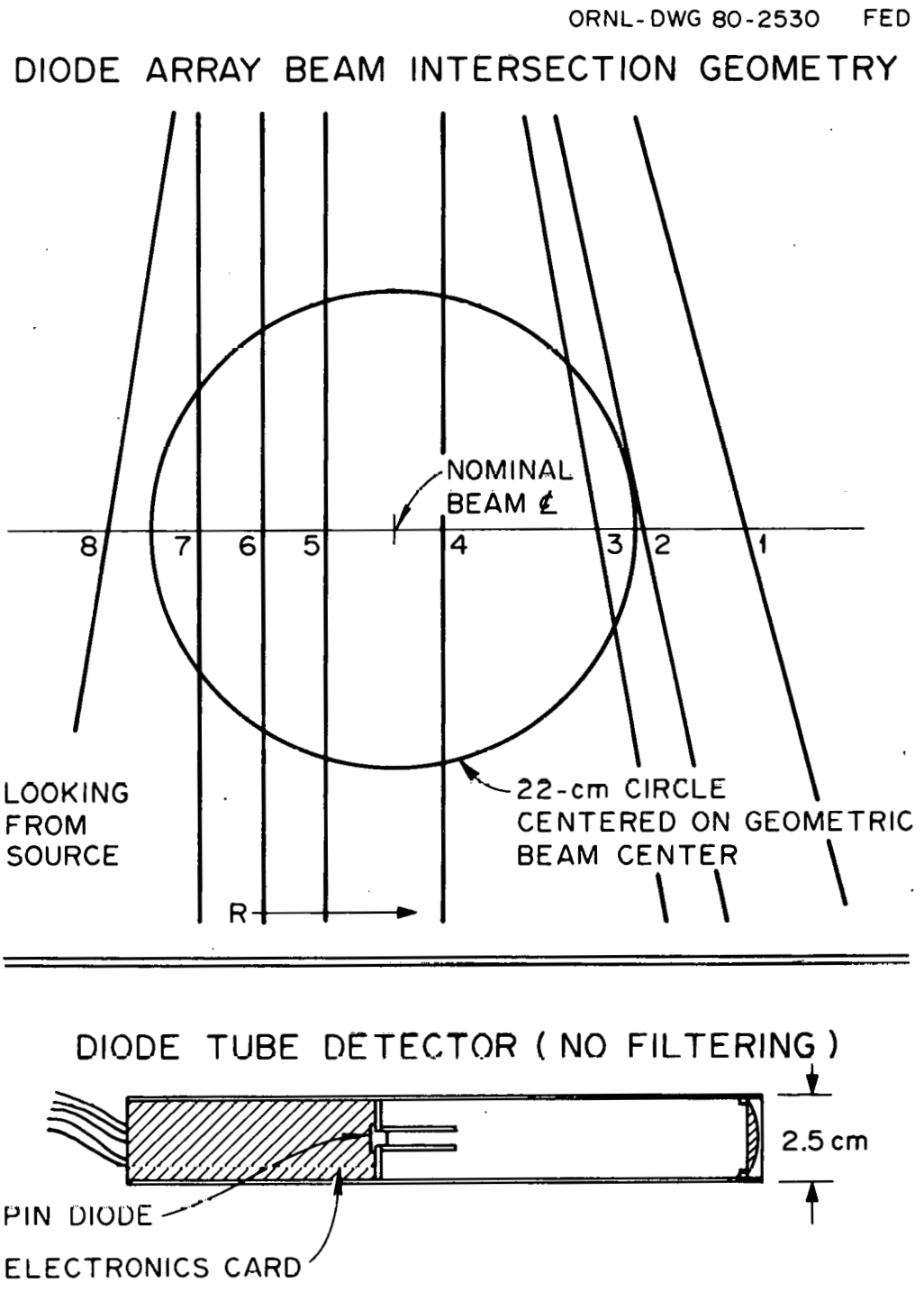

Fig. 10. Photodiode array sensor and sensor pointing.

The shot repetition rate was limited to 5-10 min by the slow time response of the target (cooling down time >100 s). Power monitor drift was checked periodically to maximize accuracy. The absolute calibration of the power monitors and the beam current and voltage monitors was checked during the experiments so that the deposited power measurements were shown to be consistent with each other and to be reliable.

On some shots, water flow to the target was shut off for calibration checks of the IR camera, and some extra beam pulses (not tokamak shots) to the target were done specifically for the IR camera studies.

Since the target experiment could only be done once, the studies were performed with immediate crude data analysis, and these results determined the extent and direction of the remaining experiments.

4.4 EXPERIMENTAL RESULTS AND DISCUSSION

4.4.1 Calorimetric Power Measurements

The primary goal of the Beam Target Experiment was to determine the amount of neutral power that actually reaches the ISX plasma. Prior to the direct measurement of power with a target in the tokamak, injected power was estimated by extrapolation from the power measured on the beamline calorimeter (for a beam-conditioning pulse that had parameters similar to those for injection). This extrapolation was used because it is the most reliable of a number of different ways to estimate the injected power. The primary check on this estimate consists of measuring extracted power (beam current × beam voltage, $I_b \times V_{accel}$) and multiplying by a transmission efficiency measured on the Plasma Technology test stand. The transmission losses are checked by the incomplete calorimetry on the ISX beamlines.

Thus, the Beam Target Experiment is first a comparison between the power measured by the beamline drift duct calorimeter (also called simply the beam calorimeter) and the power measured on the target. There are two principal effects involved in the transport of the beam from the calorimeter to the plasma: beamline geometry and beam optics, and interaction of the beam with the tokamak's magnetic field through the reionization of beam neutrals.

Experimental results for the ratios of target power to beam calorimeter power versus beam perveance ($I/V^{3/2}$) are shown in Fig. 11. Beam perveance is the controlling parameter for ion optics and is thus the natural parameter for beam optics and transmission. Beam calorimeter power was recorded from the last of a series of conditioning shots, after which the beam was fired at the target and the power measured. The perveance used for both is that of the *target* beam pulse (the perveances are slightly different when the tokamak toroidal field is fired).

Most evident in the data is the large scatter. Also, although the defining aperture has been set so that all of the beam on the calorimeter should reach the plasma, all of the power is apparently not collected on the target. Furthermore the discrepancy between the beam calorimeter and the target power increases as the perveance diverges from its optimum (nominally 6×10^{-6}). All of these conclusions appear valid in the context of error analysis, which is discussed in detail in Sect. 4.4.6. Studies of the beam profile (Sect. 4.4.2) indicate that the beam was slightly off center before the set of steering experiments, but the data in Fig. 11 show this to be a minor effect. It should also be noted that almost all of the data were taken at 40 kV, with varying beam current. The few shots at perveance over 6.5×10^{-6} represent shots with lower accel voltage; there is inadequate information to analyze these data.

Figure 12 shows that the beam calorimeter power alone varies with perveance, much as is shown for the test stand performance (Fig. 4) but at greatly reduced power. This inefficiency will be discussed in Sect. 4.4.5. The optimum perveance still seems to be about 6×10^{-6} $A/V^{3/2}$. These data are much less noisy than those of Fig. 11 since P_T/P_{cal} has the combined noise of P_T and P_{cal}, which are individually noisy.

The dashed line is an approximate best fit through the data, and the solid line represents a best linear fit that passes through the origin, indicating how closely the calorimeter power scales with extracted power, in this case with current, since $V_{accel} \approx$ constant.

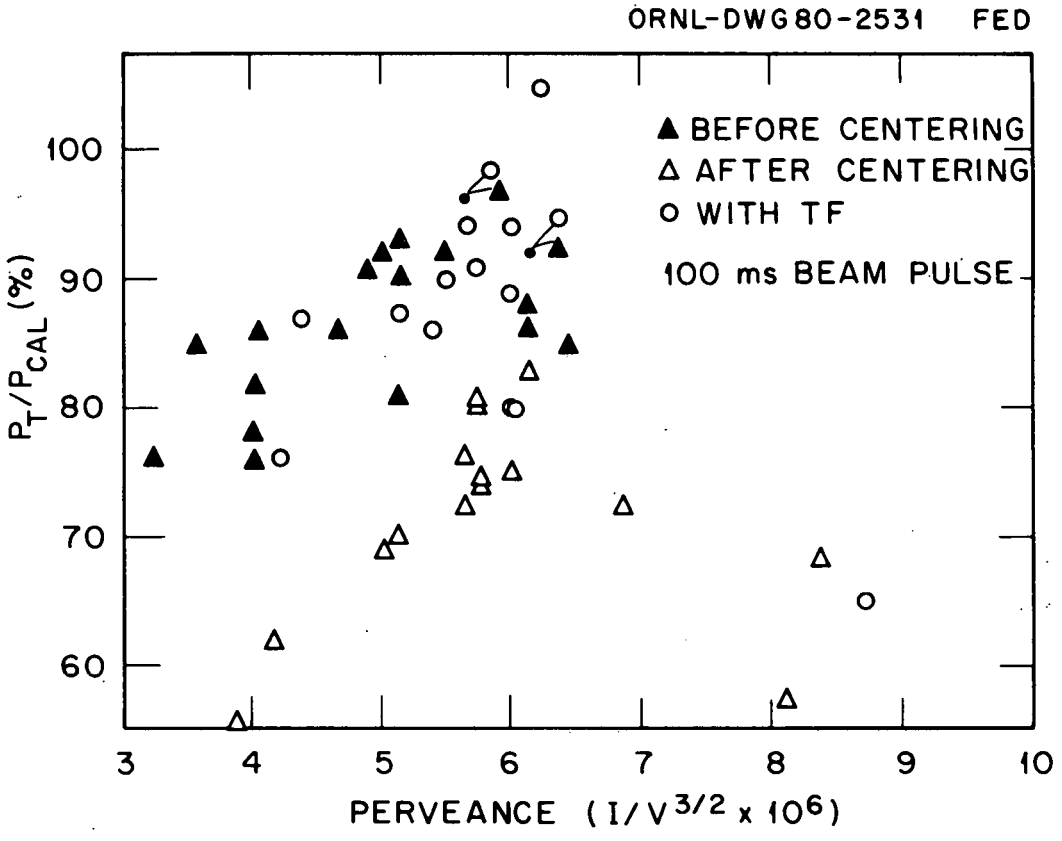

Fig. 11. The fraction of the calorimeter power that reaches the target at varying beam perveances.

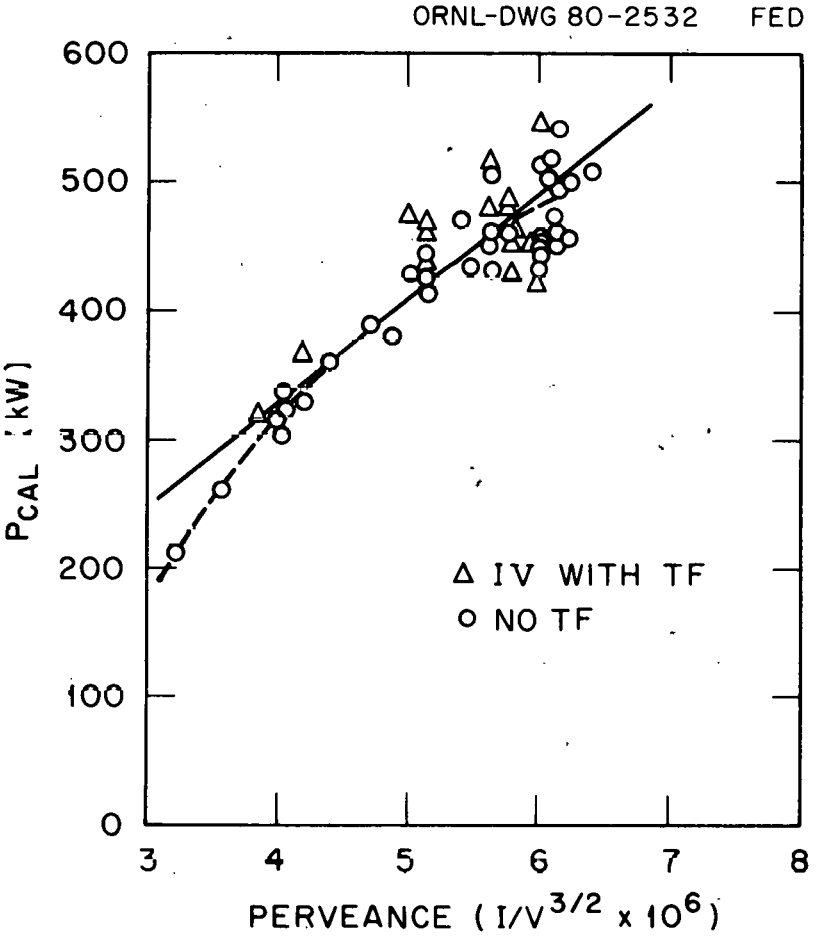

Fig. 12. Beamline calorimeter power as a function of perveance.

Thus, within this range of perveance, the effect of beam optics on the beam calorimeter power is minor, perhaps because the optics changes primarily affect the beam edges and these have been scraped off by the defining aperture. The data also show no effect of the toroidal field on the calorimeter power, or at least that it is limited to about ±5%.

It is observed that firing the toroidal field causes a drop in the local line voltage. This, in turn, causes a drop in both the accel voltage and arc voltage. The drop in arc voltage causes a drop in arc current, which results in a drop in beam current for settings that would give a higher current otherwise (i.e., for calorimeter-conditioning shots). Independent data show this effect to be about a 5% reduction in beam current and a few percent reduction in accel voltage. The effect is applicable to the data in Fig. 11 since P_{cal} is measured during conditioning without toroidal field and $I/V^{3/2}$ is measured with a toroidal field when it is fired. Since perveance is the ratio of beam current and voltage, the reduction in both quantities tends to give the same perveance, so that the change is hidden in the noise, as would be expected. The line-loading effect is thus masked by the perveance parameter, but this effect will be seen later by comparing beam power with and without the tokamak toroidal field.

The power on the target, shown in Fig. 13, behaves similarly to the beam calorimeter power, except that the power is further reduced. There is power lost between the beam calorimeter and the target without a toroidal field, and even more is lost with a toroidal field. The target power is still proportional to the extracted power at higher perveances, while optics effects become dominant far from optimum perveance. The two x's demonstrate that at higher gas pressures (i.e., large tokamak gas puff), power to the target is significantly reduced by reionization losses.

With some hesitation considering the errors involved, the table below can be made up from the data indicated by the dashed curves.

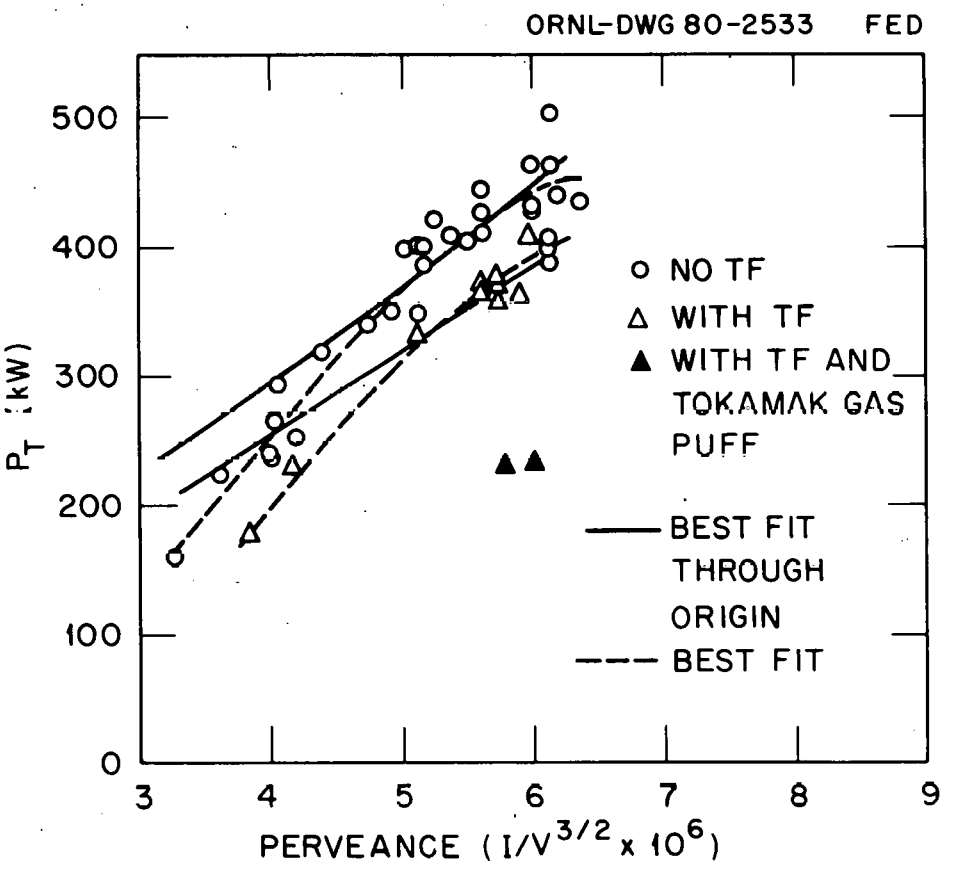

Fig. 13. Target power as a function of perveance.

Perveance ($\times 10^6$)	6.0	5.0	4.0
P_T/P_{cal} with no TF (%)	91	89	79
P_T/P_{cal} with TF (%)	81	77	63

Aside from systematic errors, these percentages could easily be ±5% off due to noise. There are two known systematic errors that cause these estimates of the power reaching the plasma to be low. The first is that the target does not intercept all of the beam entering through the tokamak port because the plates are not large enough. The second is that during a plasma shot the edge pressure is very low; this would reduce the background pressure in the drift duct and hence the reionization losses from the beam. Both of these effects will be discussed and estimated in Sects. 4.4.3 and 4.4.4, respectively.

4.4.2 Beam Intensity Profile Measurements

Three techniques were available to measure beam intensity profiles at the target. The thermocouples in the target measured the deposited energy transferred through the plates on a long time scale, giving point measurements of the time-integrated beam profile. The IR camera, by continuously scanning across the target surface, gave time-integrated profile information both during and after the beam pulse. In addition a photodiode array gave line-integral profiles of the radiation from the beam passing through the background gas in front of the target.

Of the three techniques, the thermocouple array gives results that are the most accurate and the most easily interpreted. In Fig. 14a the thermocouple data are compared to the IR camera data. The two measurements agree very well. Unfortunately the IR camera was not set up to take quantitative data; most of its information is in the form of photographs of the camera output of the entire target surface at one instant. Some line scans were taken, giving the data in Fig. 14a. Thus, the IR camera is used primarily to check the thermocouple results. Figure 14b (upper graph) shows a comparison between the thermocouple results and

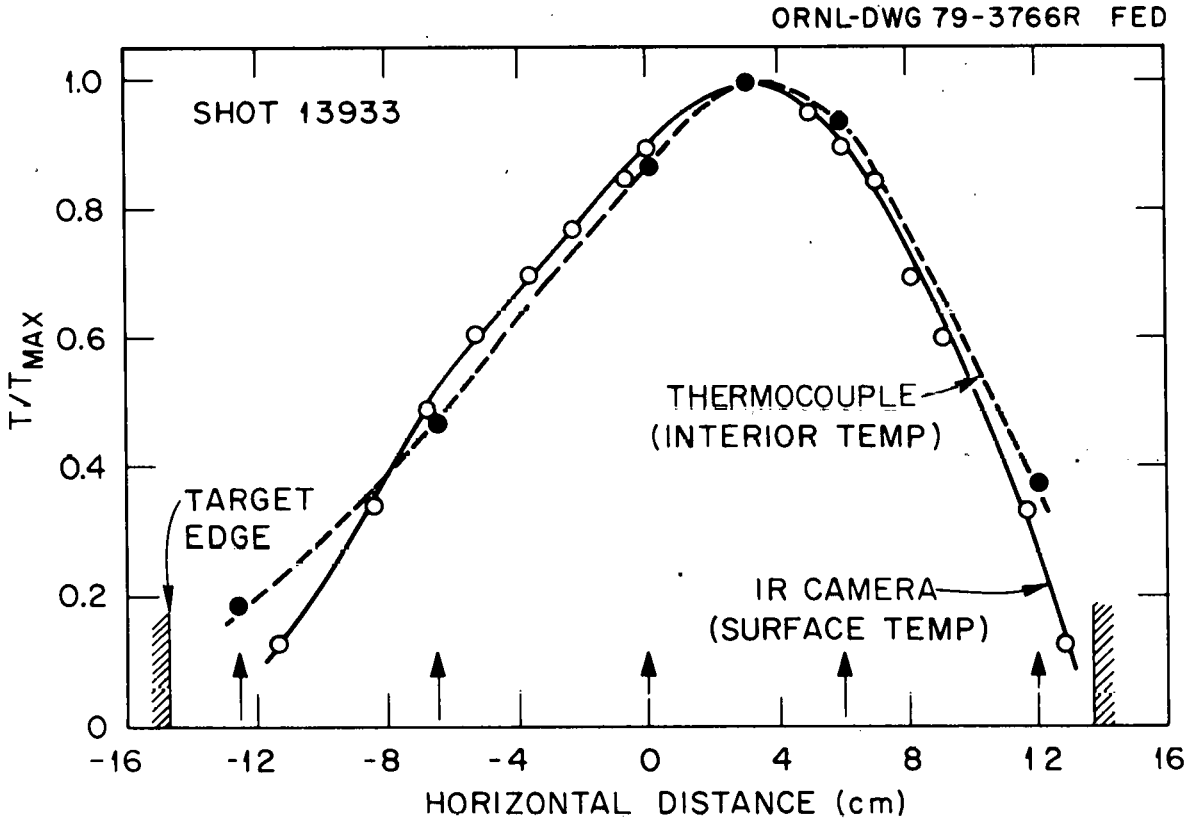

Fig. 14(a). Comparison of IR camera data with target thermocouple data.

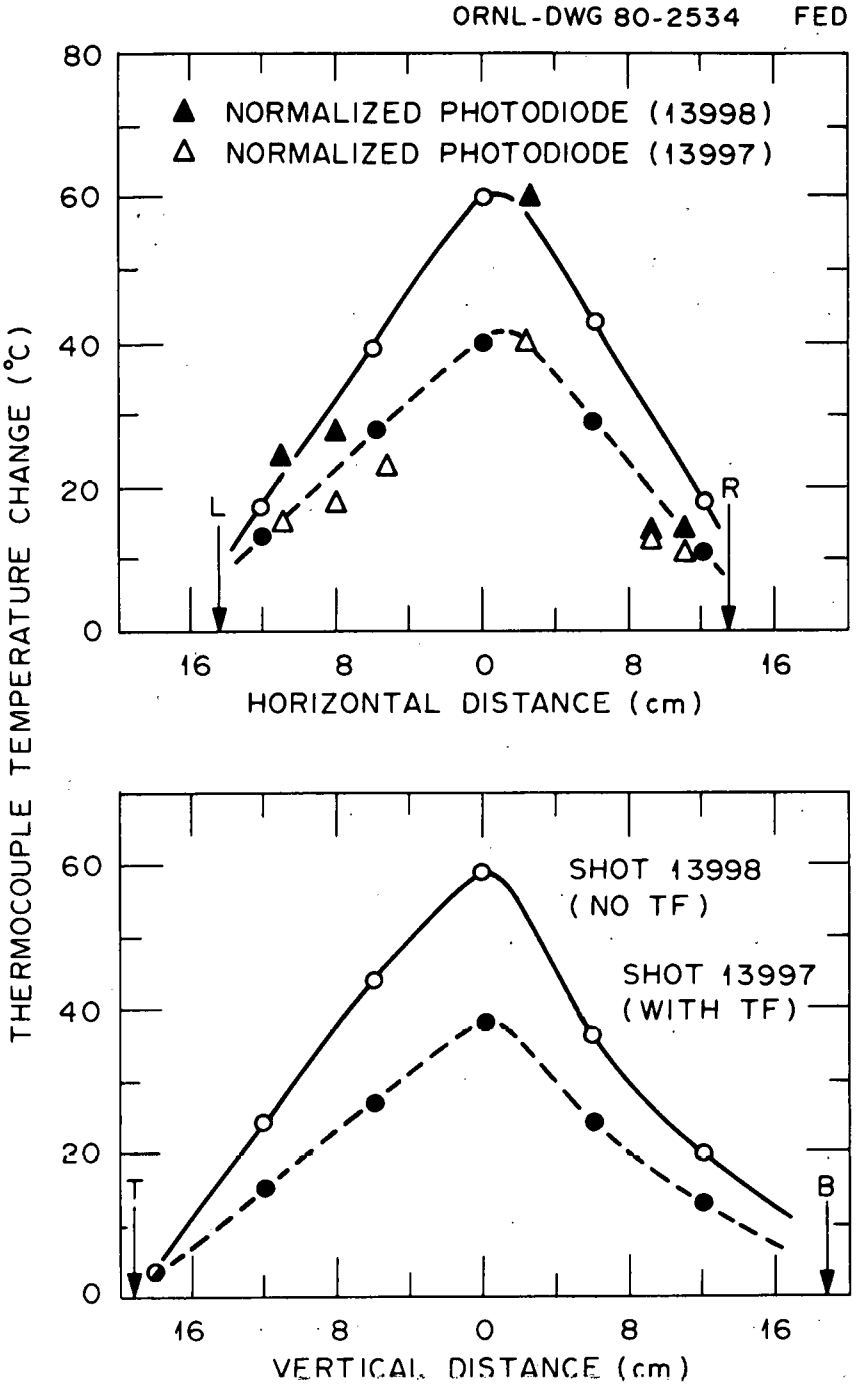

Fig. 14(b). Comparison of photodiode array data with thermocouple data.

the photodiode data, where the latter profile is normalized to the peak temperature change of the thermocouples. The agreement here is not very good for two reasons. First, the photodiodes sense the product of the beam intensity and the background gas density. During a beam pulse, outgassing from the target makes a significant contribution to the signal (superimposed on the tokamak gas puff) and increases with time; the effect is intensified in the center of the target, which is hotter. Furthermore the beam profile is not Gaussian, and care must be taken in comparing point profiles with line-integral profiles. However, the two profiles do seem to be consistent. The photodiode data will be used primarily for examining time-resolved profiles from shot to shot as a relative measure of different effects. The photodiode array looks in front of the target from above and slightly behind it, so that the surface itself does not contribute to the emission.

Figure 15 compares the theoretically predicted profiles[3] to those measured by the thermocouples. Although the fit is not bad, two aspects stand out. First, the actual profiles are narrower than those predicted. It would be expected that various defects in the source optics would contribute to a defocusing of the beam and thus a larger half-width. Second, there is a marked asymmetry in the beam profile, especially in the vertical direction. This same vertical asymmetry also shows up clearly in the IR camera photographs of the target. It is likely that these two effects have a bearing on the overall poor performance of the beamline; this is discussed further in Sect. 4.4.5.

Figure 16 shows the results of a source-steering scan. The source was rotated about a vertical axis by a gimbal controller, so that the center of the beam moved across the target to the right. The two profiles compare the data for a centered beam with that displaced about 6 cm to the right horizontally. Note the arrows on the graphs that indicate the location of the target edges.

The behavior of the profiles is strongly affected by the beam-defining plates, which cut off the beam edges with an 18-cm-square aperture as the beam converges from the source. The normal edges of the beam are shown by the horizontally misaligned profile, indicating that there is a central portion of the beam with an exponentially decaying

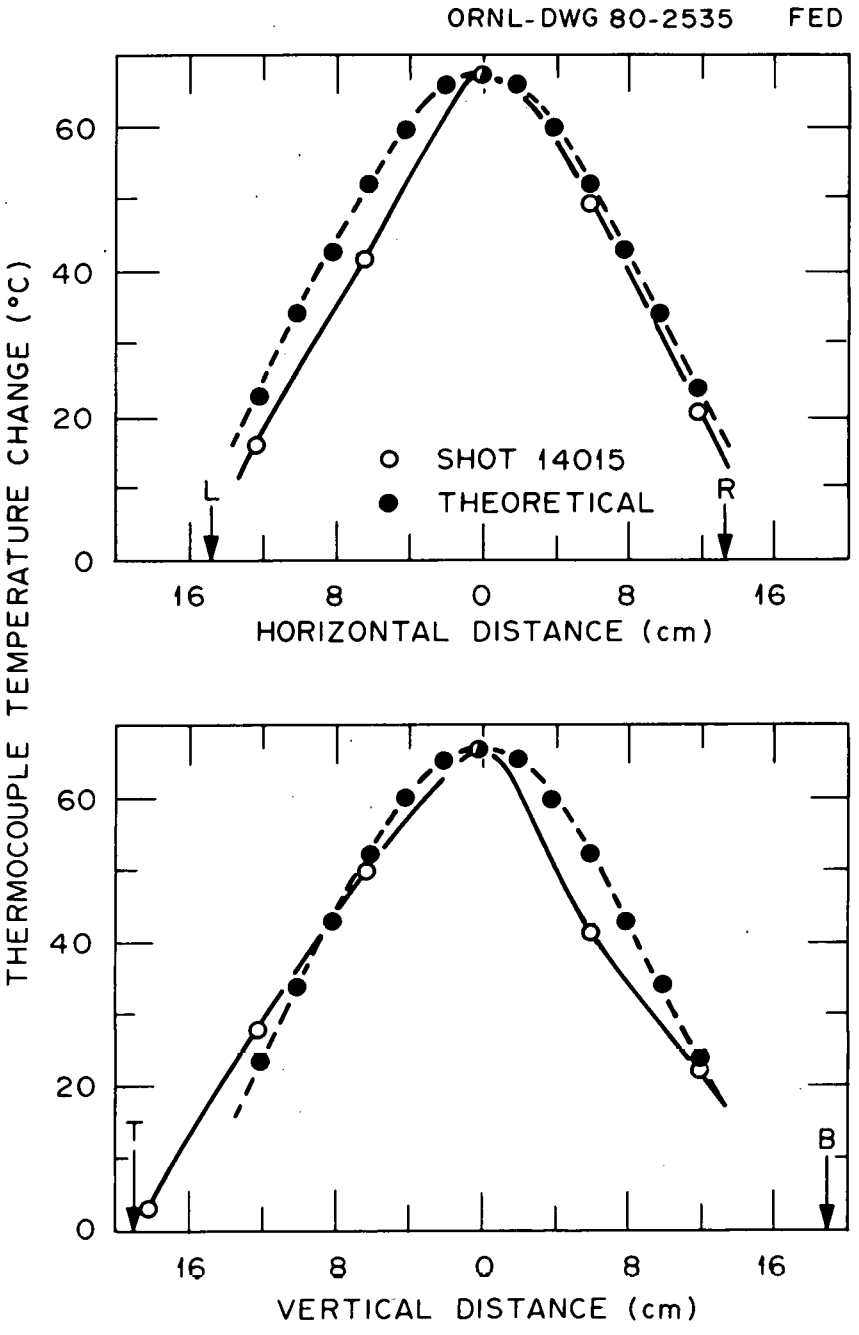

Fig. 15. Comparison of thermocouple data with theoretically derived profiles.

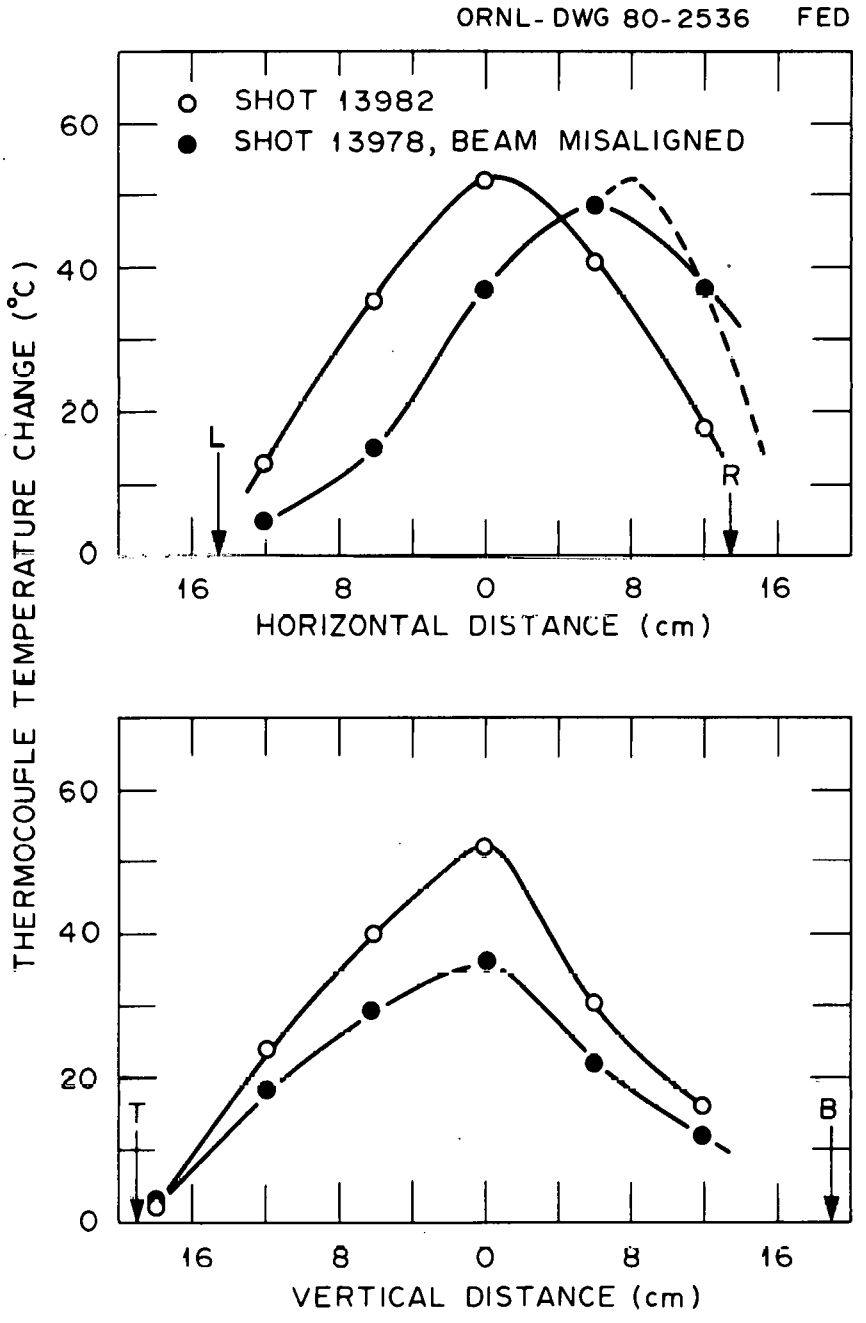

Fig. 16. Thermocouple data beam profiles comparing a well-centered beam with one steered to the right.

edge. A significant part of the beam is outside the tokamak port radius of 14 cm, but it is uncertain how much of this tail is cut off by the defining plates. The vertical profiles indicate that there is still a significant part of the beam that hits the drift duct walls, since the beam edges have filled it out to an 18-cm radius.

The off-center beam also seems to have a slightly lower peak intensity, but a fit to the data of the dotted line, giving the same peak intensity, is more probable. Finally, the vertical profiles indicate that the beam is asymmetric about the horizontal plane, rather than rotationally asymmetric. The two profiles are parallel vertically but offset horizontally, and the similarity between the two implies that something is probably wrong with the bottom half of the source. The IR camera data also show this kind of asymmetry.

Figure 17 shows the effect of the beam perveance on the beam profile. Shot 13964 has a perveance of 6.1×10^{-6} $A/V^{3/2}$, while shot 13968 has a perveance of 3.2×10^{-6} $A/V^{3/2}$; the latter should represent optics far from the optimum. The profiles indicate two different results: the vertical profiles are very similar in their central portions, and the horizontal profiles indicate that the profile has skewed to the right. These results hold over a range of perveances, again implying important noncircular asymmetries in the source.

Finally, Fig. 18 shows the profiles resulting from shots with identical conditions except for the presence or absence of the tokamak toroidal field. The shape is unchanged although the beam intensity is reduced. These data are taken without a tokamak gas puff. A similar result holds for a large gas puff, as shown in Fig. 14b, although the power to the target is reduced by almost half. From this it is concluded that the beam neutrals lost through reionization are lost in direct proportion to the beam intensity and are swept entirely away from the target. Most of this loss is in the drift duct; the ions are swept into the drift duct walls.

An additional piece of information about the source optics arises from the fact that the beam profiles remain unchanged in shape when the pulse length is changed from 100 ms to 200 ms, implying that grid shape changes due to heating are unimportant at these power levels.

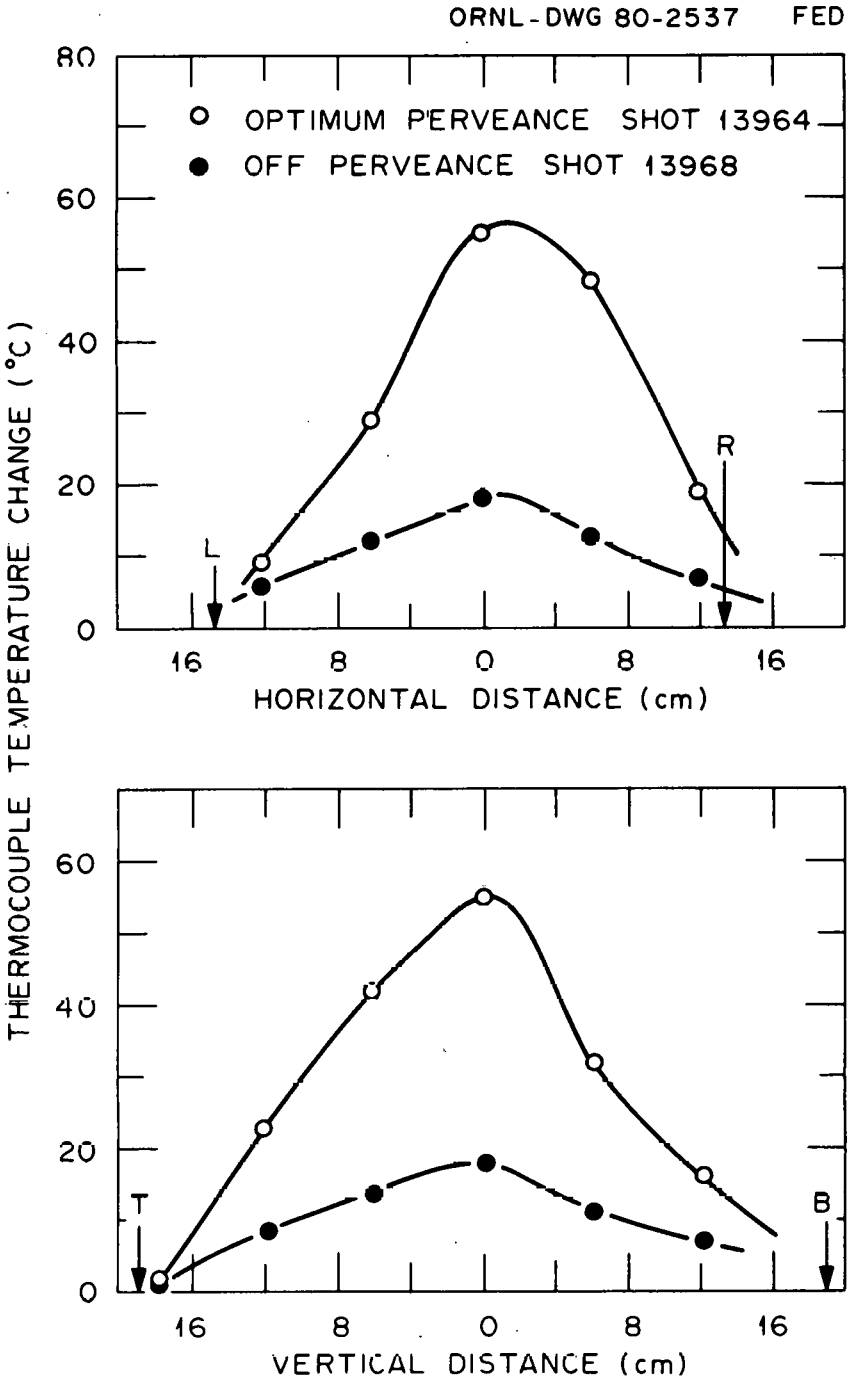

Fig. 17. Thermocouple data beam profiles comparing a beam at optimum perveance (6×10^{-6} A/V$^{3/2}$) with one at off perveance (3×10^{-6} A/V$^{3/2}$).

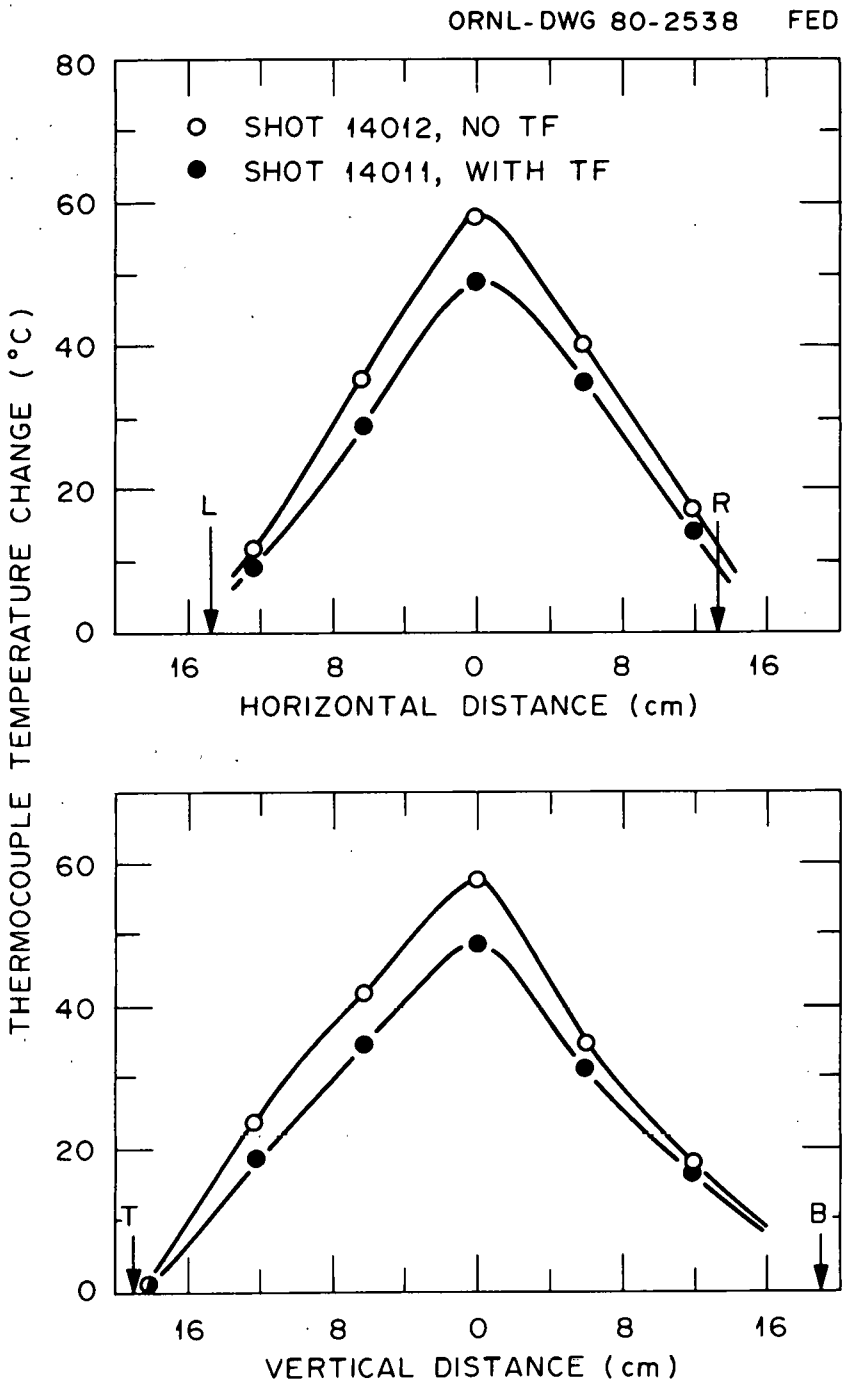

Fig. 18. Thermocouple data beam profiles comparing beam pulses identical except for the presence or absence of the tokamak toroidal magnetic field.

4.4.3 Optics Losses

Two questions are to be addressed in this section. First, what fraction of the beam power is lost due to direct collision with the drift duct walls? Second, the West beamline, used for this experiment, was operating with optics measurably different from a nominal beamline. What would the optics losses be for nominal optics?

The first question is complicated by the limited size of the target. Figures 12 and 13 indicate that between about 10% and 20% of the calorimeter power is not collected by the target; the discrepancy increases as the beam departs further from its optimum perveance. Away from optimum perveance the profiles are flatter, and thus the amount missing the target should be a higher fraction of the total power, as would be true of the fraction of neutrals hitting the walls. This accounts for the increased loss with perveance.

Even though the width of the target plates together is the same as the diameter of the tokamak entry port, it is evident from both the vertical and horizontal beam profiles that some power misses the target. This, together with the power lost through a small crack between the paddles, is estimated to be approximately 5% at optimum perveance. This estimate is derived from calculations of Gaussian profiles approximating the true profiles. Thus, given experimental accuracies, the beam power lost to the drift duct walls should be from a few percent up to perhaps 5% of the beam power at optimum perveance. Both of these losses should increase to about 10%, far from optimum perveance; this accounts for the power losses implied by Figs. 12 and 13.

The second question, that of geometry losses with nominal beam optics, is best answered by relying on test stand data. There geometry losses are insignificant; the defining-plate aperture size has been determined to make this so. Thus the explanation of the particular beam optics behavior seen in the Beam Target Experiment is that the central portion of the grids has optics closer to nominal than the outside, so that more of the central beamlet portion of the beam gets to the target, while the outer part diverges more. This results in a narrower beam profile than normal, but more geometric losses, as is seen in the

experiment. With a nominal source, the beam profile should be broader, but the geometric optics losses should be less due to lower divergence.

4.4.4 Reionization Losses

The essence of neutral beam heating of tokamak plasmas is the addition of high-energy particles to the plasma. These particles must begin as neutrals outside the tokamak so that they can pass through the magnetic fields that confine the plasma itself. Once these neutrals reach the plasma, they are collisionally ionized and trapped in the torus plasma, gradually transferring their energy to the surrounding plasma and heating it. If there is some background gas in the path of the neutral beam before it reaches the tokamak, some of the high-energy neutrals will be ionized and forced out of the beam by the tokamak magnetic fields before they reach the plasma. This loss of neutrals, and thus neutral power, is known as reionization loss — reionization because the beam is first generated by neutralizing an accelerated ion beam.

Reionization losses will be discussed here in some detail. Data from relevant experiments have led to the conclusion that reionization losses are indeed present in the ISX beamlines but that, contrary to expectations, the background gas arises from normal beamline gas flows, rather than wall outgassing.

In the absence of gas flow from the tokamak to the beamline (the plasma pumps gas at its edge), background gas in the beamline can come from wall outgassing, inadequate pumping of the normal beamline gas flow, the buildup of stray particles from the beam itself, or any combination of these. Each of these gas sources has a characteristic signature in terms of its effect on the beam and the beamline. Typically, wall outgassing occurs because the wall is heated by some beam neutrals. In addition, the reionized beam particles are deflected to the drift duct walls, causing more local heating, more outgassing, and a higher background pressure with more reionization, in an accelerating process that can lead to catastrophic beam loss. This case would imply a

monotonically increasing drift duct pressure and a monotonically decreasing beam transmission to the plasma.

Chronologically, the first information about the magnitude and mechanism of reionization came from a short experiment performed on the West ISX beamline earlier in 1979 (unpublished), without a target. In this experiment the beam was fired into the tokamak after a background gas pressure had been puffed into the torus with the gas injection system normally used to fuel the plasma. The diagnostics used were the photodiode array (the same as used in the target experiment) and a photodiode that looked at the beam as it emerged from the gas cell in the beamline. By comparing these signals with and without a tokamak toroidal field present, reionization losses could be estimated. There were two levels of gas pressures used; these were identical to those used in the target experiment.

The results from this experiment indicated that reionization losses were not important, that the effect was on the order of 20% or less even at the higher of the two pressures examined. The accelerating effect of outgassing from the drift duct was shown to be negligible by noting that the ratio of the photodiode array central channel to the beamline photodiode showed no time dependence in the presence of a toroidal field (Fig. 19). It should be noted, however, that for a tokamak plasma shot, the reionized neutrals first encounter stray poloidal magnetic fields rather than the toroidal field. This difference in the location of the deposited ions is not thought to be significant for the ISX beamlines.

The presence of reionization losses due to a steady-state background gas pressure, presumably caused by the gas puff in the tokamak, was assessed by comparing the array data with and without the toroidal field. Interpretation of the results is complicated by different beam powers from shot to shot; these could be normalized to first order by comparing the beamline photodiode signals. The two tokamak pressures differed by a factor of 2. At the higher pressure ($\approx 10^{-3}$ torr) the data imply a 15-20% loss; at the lower pressure the loss is not obvious, but could be as much as 5%.

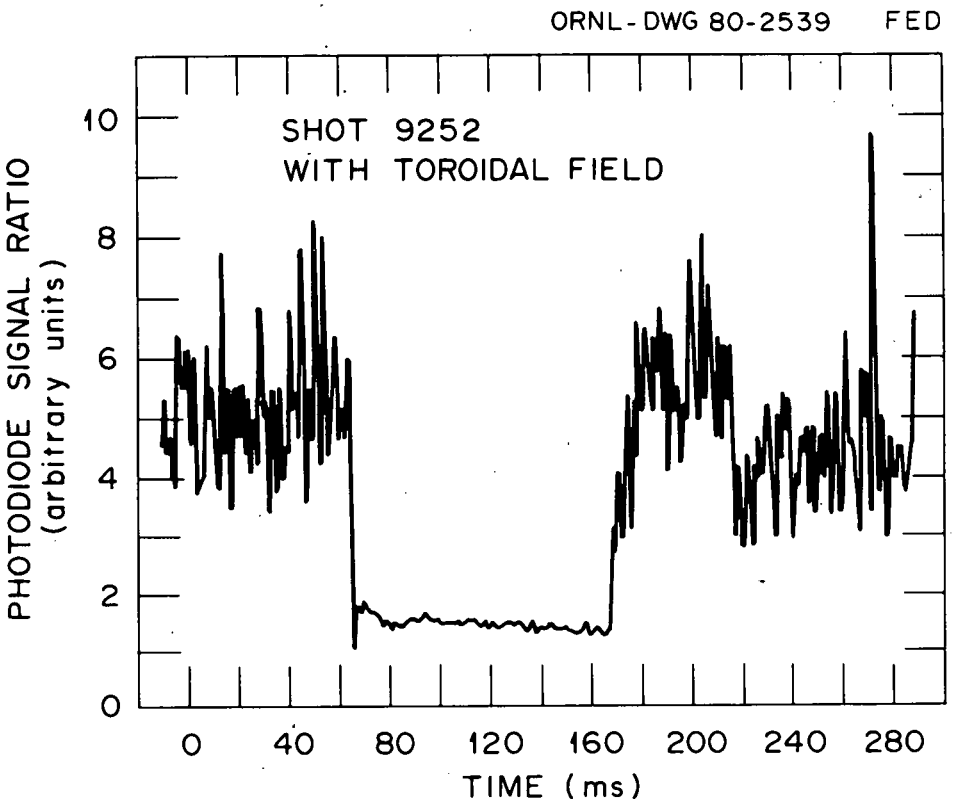

Fig. 19. Ratio of beamline photodiode signal to target photodiode array central channel signal indicating no difference in beam intensity time history at the two locations.

The experiment was done in February 1979 and the data were very reproducible at the time. The photodiodes and gas puff system were unchanged between then and the target experiment, but the beamline performance did change, and in a major way; this problem is discussed in Sect. 4.4.5.

Results from the target experiment give reionization losses that are significantly different from the preliminary tests discussed above. Significant reionization losses were seen in the absence of tokamak gas puffing, while the gas puff tests at the higher pressure showed losses of about 40% (see Fig. 13). Analysis of all of the target experiment data implies that the reionization mechanism was the same; the source performance changed, leading to different reionization losses.

In Sect. 4.4.1, the calorimetric data as a whole implied a variation of P_T/P_{cal} with perveance and with the presence or absence of a toroidal magnetic field. As our discussion here shows, a change with and without toroidal field implies reionization losses. These were seen to vary from 10-15% of the beam power on the calorimeter as the beam optics diverged from optimum perveance. With the tokamak gas pressure at its higher value from the gas puff, the power to the target (two data points) was reduced by about 50%, or 60% of the calorimeter power.

These data do *not* include the effect of the electrical loading of the beam power supply by the toroidal field supply. That effect was taken into account by plotting the perveance of the beam during the toroidal field pulse (when it was present). Thus for the same nominal beam settings, a beam pulse with a toroidal field is reduced in both power and perveance; the effects offset each other only for constant beam voltage, the case here.

The background gas source, whatever it is, must then account for reionization of about 10% of the beam, in the absence of a tokamak gas puff.

Unlike the first experiment, the raw photodiode data taken during the target experiment show a different time dependence than that of the beam pulse itself. Typical data are shown in Fig. 20a-f. These data are plotted on the same scale as those shown in Fig. 20g for the previous experiment, for the same gas puff as used in Fig. 20b. There is an

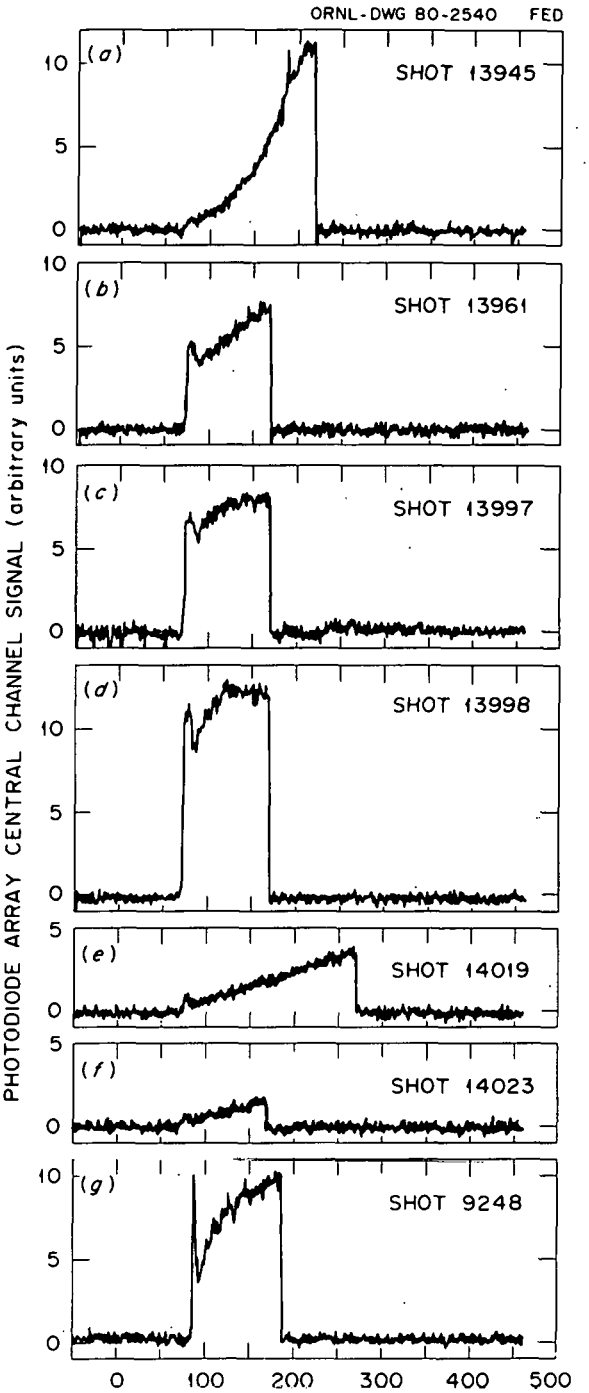

Fig. 20. Photodiode array central channel data: (a) an early shot in the beam target experiment, (b)(d) later shots with tokamak gas puffing, (e)(f) shots near the end of the experiment, and (g) a beam pulse into gas with no target during an earlier experiment.

exponentially increasing signal from gas present without a gas puff in the tokamak; the two signals are superimposed in the presence of a gas puff. It should be noted that due to the configuration of the photodiode amplification electronics, the incident light intensity is proportional to the signal voltage V (plotted) to the 1.4 power.

One obvious difference between the two experiments is the presence of the target. Although the target had no effect on the gas pressure as an obstruction, there was no question that its surface outgassed significantly when it was being heated by the neutral beam. The photodiode array was mounted directly above the target and was slanted to take a profile about 10 cm in front of it. The array was thus very sensitive to target outgassing, unlike the pressure in the drift duct. In fact, it can be shown that without a tokamak gas puff almost all of the photodiode signal comes from target outgassing.

Without a gas puff, gas contributing to the signal must come either from target outgassing or from the beamline itself. The target plates were only cleaned, not baked, so one would suspect a large outgassing rate from the surface when its temperature is raised to hundreds of degrees Celsius by the beam. The plates are made of ordinary 304 stainless steel.

The progressive outgassing of the target can be traced throughout the experiment. Figure 20a shows the rapid rise in signal of the central channel of the array for a shot early in the experiment. At the end of the second day of the experiment, the beam was pulsed onto the target without the deflection magnet on, and it deposited about 60% more power on the target than the previous maximum; the thermocouples inside the plates recorded a similar 60% increase in peak temperature. Subsequent shots (Fig. 20b) showed a much smaller rise in the signal. At shot 13988, the degassing process was nearly completed by a mistaken multiple (4) pulse of this type shot, causing an *internal* temperature rise of almost 300°C compared to a more typical 50-60°C. The outgassing signal was almost negligible for a similar 200-ms shot (Fig. 20e) at the end of the experiment. The residual outgassing at the end of the experiment is shown in Fig. 20f, at a typical beam power. When the effect of outgassing

from the target is subtracted, these results are then similar in form to those of the earlier experiment.

That the drift duct outgassing did not contribute significantly to the pressure rise or to beam reionization can also be demonstrated. After the target had been essentially baked out by beam shots, a 200-ms shot (similar to Fig. 20e) without the ion deflection magnet on was pulsed onto the target. This beam, with 30-40% ions, was fired with and without the toroidal field. Assuming a typical 10% reionization, these shots caused a wall heat loading that was at least a factor of 3 or 4 higher than normal. At these increased ion fluxes, no change was observed in the photodiode signal. A signal increase would have indicated more pressure in front of the target; a decrease would have indicated greater reionization losses due to an increased pressure in the drift duct (but not at the target). Thus for the particular conditions on ISX, drift duct outgassing is unimportant.

All of the evidence indicates that there are minor reionization losses that are not time dependent. This rules out beam heating effects and implies that the background gas source arises from normal beamline gas flows that have reached equilibrium before the beam itself turns on. The discussion below is an attempt to show that this is consistent with known beamline conditions.

Complicating the understanding of the reionization gas source is the fact that the pressures in the beamline are highly nonuniform. Not only are there pressure gradients of orders of magnitude in the beamline and the tokamak, but there is also molecular streaming along the direction of the beam inside the beamline.

There are a number of gas sources and sinks in the beamline tokamak system. Neglecting wall pumping, the gas sinks are the tokamak vacuum pump (turbopump $\approx$ 500 liter/s), a beamline cryocondensation pump ($\approx$200,000 liter/s), and the plasma when it is present. The tokamak and beamline have their own volume time constants, and there is a conductance between the tokamak and beamline set by the drift duct geometry. Gas is supplied to the system from the ion source and gas cell, the tokamak gas puff, and any wall outgassing that may occur during the beam.

The time scales involved for ISX plasma shots are on the order of 100 ms, and the volume of ISX is about 500 liters, so that the 500-liter/s pumps have a negligible effect during a shot. In the beamline the ion source gases are turned on 100 to 200 ms before the beam pulse so that the pressure has reached equilibrium with the cryopumps by the time the beam is fired. This equilibrium is changed by the beam both in the source and in the beamline as a whole.

Beyond this description, it becomes difficult to specify the gas distribution because of a lack of experimental data. Because of the high pressure gradients in the beamlines the physical location of any pressure sensor is very important. Measurements on the Medium Energy Test Facility beamline[7] indicate that the pressure in the main beamline tank is 1-2 $\times 10^{-4}$ torr (30-A, 40-kV beam), while the gas cell pressure is $\approx 1 \times 10^{-3}$ torr. Presumably the background pressure that the beam passes through is somewhere between these pressures, because of the streaming of the gas along the beam and the reduced pumping due to shielding by the magnet that surrounds the beam to deflect the ions.

The drift duct pressure will probably be between the beamline and tokamak pressures. For a typical injection shot the pressure will not be in equilibrium, since on the tokamak side it begins at low pressure ($<10^{-5}$ torr), increases with the tokamak prefill gas puff (50 ms before a shot), then decreases to a low pressure again due to pumping by the plasma. Typical steady-state tokamak prefill pressures are 2-3 $\times 10^{-4}$ torr, so one would expect a drift duct pressure on the order of 1×10^{-4} torr in the absence of wall outgassing.

The fraction of the beam that is reionized is given by

$$\frac{I}{I_o} = e^{-n\sigma\ell} ,$$

where n = background gas density, σ = collision cross section, and ℓ = path length through the gas. For 40-keV H^0, $\sigma \approx 1.4 \times 10^{-16}$ cm^2/mol, and n = 3.3×10^{16} p (torr), so

$$\frac{I}{I_o} = \exp(-4.6\ \ell p)\ ,$$

where ℓ is in centimeters and p is in torr. Thus at a pressure of 1×10^{-4} torr and a path length of 2 m (the length of the drift duct in ISX), 10% of the beam is reionized.

This is in good agreement with both the pressures that one would expect in the drift duct from the above discussion and the reionization losses that were measured in the beam target experiment. *However*, it is important to note that these conditions are very near the transition from linearly increasing to exponentially increasing reionization; that is, any increase in pressure will cause a much larger reionization loss. This explains why the earlier experiment (with nominal beamline operation) showed small reionization losses compared to the Beam Target Experiment; part of the beamline inefficiency was reflected in higher beamline pressures and thus higher reionization losses.

To summarize, the conclusions from the reionization data on the ISX beamlines are:

1. Reionization losses due to drift duct outgassing are negligible (500 kW, 100 ms, ISX geometry).
2. Reionization losses are present on the order of 0-10% due to background pressure in the drift duct.
3. The normal background pressure causing reionization is such that the additional gas from other sources will have a disproportionally large effect on the reionization.

One final piece of confirming evidence is that in a short sequence during the experiment, the reionization losses were found to increase with increasing gas cell pressure while all other beam conditions were fixed.

4.4.5 Applicability of the Beam Target Experiment

As with present-day tokamaks, the behavior of the beamlines on ISX is very dependent on small details of the beamline itself. The transfer

of neutrals to the plasma is dependent on both the optics of the beam and the presence of a background gas, from whatever source.

The first question to be addressed is the extrapolation of the performance of the West beamline during the Beam Target Experiment to all other injection on ISX. At the time of the experiment, the West beamline source was delivering significantly reduced power compared to its test stand operation at the same parameters. This degradation was only noticed after it had occurred, and little information is available about the process or the cause. Although peak performance was originally 900 kW, by July 1979 it was 650-700 kW.

This inefficiency was reflected in a poor beam optics (seen by the beam profile measurements) and a higher beamline pressure (deduced from two reionization experiments). These effects, in turn, should cause higher geometry losses and higher reionization losses than a nominal beamline. Since both of these losses are small (≈10% or less) and the difference in the effects from a nominal beamline is known as far as the transfer of neutrals is concerned, ISX injection estimates based on these results should be valid in general, with minor corrections.

The extrapolation of these results to beamlines in general is probably not valid. Not only are pressure distributions poorly known and understood, but this experiment has been found to be very sensitive to changed gas flows. The interaction between beamline geometry and beam optics and transmission is also very dependent on the details of the beamline and source operation.

4.5 CONCLUSIONS

The Beam Target Experiment was a definitive test of injection power estimates on ISX. It quantified the loss mechanisms involved and clarified the errors inherent in the beam diagnostics.

In predicting injected power from that measured by the drift duct calorimeter during a conditioning shot, three important effects were measured. The first was electrical loading on the beamline power systems by the tokamak toroidal field. This caused a beam power drop of 7-8% from that measured on a calorimeter-conditioning shot. This

effect is real because the injection beam parameters are fixed by the maximum reliable *conditioning* parameters. Secondly, a small amount of geometric beam blocking was found due to beam divergence in the drift duct. The blocking was 0-5% at optimum perveance (6×10^{-6} A/V$^{3/2}$) and 5-10% at the worst practical operating perveance (4×10^{-6} A/V$^{3/2}$). The last and most important effect is that of reionization beam losses; some of the beam neutrals are ionized and ejected from the beam path. Reionization losses were found to be 10-15% of the calorimeter power at optimum perveance and 15-20% at the worst practical perveance (as above). The reionization was caused by the background gas in the drift duct arising from normal gas flow within the beamline ($\approx 1 \times 10^{-4}$ torr).

These are the results of the target experiment; they must be modified slightly to make general predictions of injected power into a typical ISX plasma. First, injection is almost always done near optimum perveance at all power levels. Second, during a plasma shot the pressure at the end of the drift duct is very low; this should reduce the reionization losses slightly.

Thus injected power should be about 85% of that measured on the beamline calorimeter. Slightly less than half of the reduction is due to the toroidal field loading; slightly more is due to the reionization losses.

These results hold only for the conditions present on ISX-B up to 500 kW injected in 100-ms pulses and the particular geometry of the ISX beamlines and sources.

The writing of this report has made it very clear that there are several areas of neutral beam work that desperately need experimental input. These are: beamline pressure measurements, long term (months/years) source behavior, and beamline diagnostics in general.

THIS PAGE

WAS INTENTIONALLY

LEFT BLANK

Appendix A

EXPERIMENTAL ERROR

The Beam Target Experiment was done at two different levels. The first considered total beam power and its transmission to the plasma from the ion source. For this purpose there are very few crucial parameters: the beam current I and voltage V, and the power measured by the beamline calorimeter and the target. The second level concerns the beam profile measurements by the thermocouples, the photodiodes, and the IR camera. The accuracy of all of these measurements will be discussed.

Of the basic parameters, conceptually the simplest is the beam voltage V_{accel} measured by a voltage divider. High-voltage dividers (100 kV) are subject to current leakages and pulse compensation subtleties, but these problems have been overcome to give an accuracy of a few percent. The beam current, that drawn by the beam from the high-voltage power supply, was measured by an induction current sensor. The sensor was calibrated with a current shunt during the experiment. The calibration was confirmed during later operation by comparison with a different type of sensor used at the same time. The primary statistical error in this measurement is about 5% due to a 60-cycle ripple superimposed on the signal. Data on both I and V were read off of oscilloscope photographs, giving the extracted power an error on the order of ±10%, including reading and averaging (over a beam pulse) errors.

Power measurements actually consist of an electronic calculation of the energy deposited in water-cooled plates hit by the beam. The flow rate of water to each plate, together with its temperature rise, is measured by a flow meter and a thermocouple block, respectively. The product integrated over time and multiplied by the appropriate constant gives a result in kilojoules of deposited energy. This number is calculated by the power monitor circuit and the result is displayed digitally. This technique is described in detail elsewhere.[8] Since the beam pulse length is usually 100 ms and the pulse shape is square, the displayed number is usually read as a power with the appropriate decimal point.

Errors that arise in this measurement come from the electronics itself as well as the inaccuracies of the flow and ΔT measurements. The latter are accurate to a few percent delivered from the manufacturer, in the regime in which the thermocouples are used. The accuracy of the flow meters depends on the flow passages being properly designed to reduce turbulence. The output signal of the ΔT thermocouples was on the order of microvolts for the flow rates used in the calorimeter, resulting in significant drift in the amplification electronics over a time scale of minutes. The flow rates were much lower in the target and ΔT was consequently higher; thus, for the target power, drift error is unimportant. These drifts were checked periodically throughout the experiment; errors from this effect were 5% or less for the beamline calorimeter and unimportant for the target power.

A possible source of error is the method of integrating the power from each beam pulse. The target calorimeter simply integrated the energy transferred to the water over an interval of about 5 min. The beamline calorimeter, however, integrated the energy deposited for each shot above an equilibrium background level reached through a constant repetition rate. It took 5-10 good shots to reach this equilibrium. Calorimeter power would be systematically low if this equilibrium had not been achieved. Typically, however, conditioning required so many shots that this was not a problem. As a check the beam was fired singly, and the integrated energy was compared with that reached repetitively. No significant difference was found.

The largest measurement error came from miscalibration of the power monitor electronics for the beamline calorimeter. Initially there was a large discrepancy between the target and beamline calorimeter power. This problem was finally solved by the discovery, on the final day of the experiment, that the calorimeter power monitor had not been properly calibrated; true power was 72% of the displayed power. Further confusion was added when recalibration failed to change the measured power. After another check later in the day, the power dropped as it should have when the recalibration was first done.

Almost all of the calorimeter data have been corrected for this error, assuming that one calibration change was made (the last) and that

measured West beamline power was 134% of its true value for months before, back to the time it had previously been worked on. This discovery resulted in decreasing previous estimates of power injected into ISX, although the East beamline power monitor was checked and found accurate. All data are consistent with this correction. Support for the calibration correction was found when subsequent checks on the power monitor found the calibration to be stable over a time scale of months.

A fundamental problem with the power monitor calibration is that it used a voltage reference as a standard, rather than adding a known amount of energy to the water lines. This defect will be corrected for the upgraded beams.

In summary, the statistical error in the extracted power IV is about ±10% in perveance ±5% (V = constant) and about ±5% in calorimeter power. The one systematic error of significance known to be present was the positive drift of the beamline calorimeter power, but for this experiment sufficient care was taken to make this insignificant.

Of the profile measurements, the target thermocouple readings are the most accurate. The thermocouple monitoring system is a commercially available computer system that includes multiple amplifiers, analog-to-digital conversion, and a constant temperature junction box. In this system the largest error is the round-off error to the nearest degree Celsius by the analog-to-digital converter.

Both the photodiodes and the IR camera are used primarily in a qualitative or relative manner. Typical photodiode signals are measured relative to a low-level constant noise. The signal-to-noise ratio is typically at least 10:1 with gas puffing, while some information on reionization without gas puffing can be seen down to a signal-to-noise ratio of 1. The IR camera data are probably accurate to 5 or 10% as a measure of relative temperature and are used primarily as a check on the thermocouple data.

THIS PAGE

WAS INTENTIONALLY

LEFT BLANK

Appendix B

NEUTRAL BEAM UPGRADE

In the middle of November 1979, ISX-B was shut down for repairs and upgrade of various systems. Primary among these is an upgrade of the ISX beamlines from a total design power of 1.8 MW to 3.0 MW of neutral hydrogen.

The upgrade has two thrusts, one major and one minor. The major modification is a change from 22-cm ion sources at 60 A and 40 kV to 30-cm ion sources at 100 A and 40 kV. The immediate changes caused by the larger sources are a larger gas cell and a larger bending magnet. The increased power loading in the beamlines has resulted in a new design for the ion dump and a slight change in the beam-defining plates.

The more minor modification, at least in concept, is the improvement of the transmission of the beam as a whole. This is done first by shortening the entire beamline by about half a meter and second by eliminating most of the remaining length of the drift duct by replacing it with a large drift chamber in which an additional cryopump can be placed. The latter modification should make any reionization losses negligible. Finally, there is a new retractable beam calorimeter in the drift chamber. The upgraded beamline is shown in Fig. 21.

Many of the auxiliary beamline systems have been upgraded as the beamline itself was modified. New beam current sensors were installed, the cooling-water monitoring systems were redesigned and dramatically simplified, and numerous changes in the controls and instrumentation were made to facilitate operation. Foremost among the changes is the addition of a computer power monitor system. The system is described in detail elsewhere.[9] It permits shot-by-shot monitoring of all of the flows and temperature rises of the cooling water as well as recalibration of gain and zero, all through a remote terminal. Furthermore a calibration system has been built to put a known heat input in the calorimeters.

As of March 31, 1980, the upgrade modifications were complete, although the new 30-cm sources were not available due to delays in the

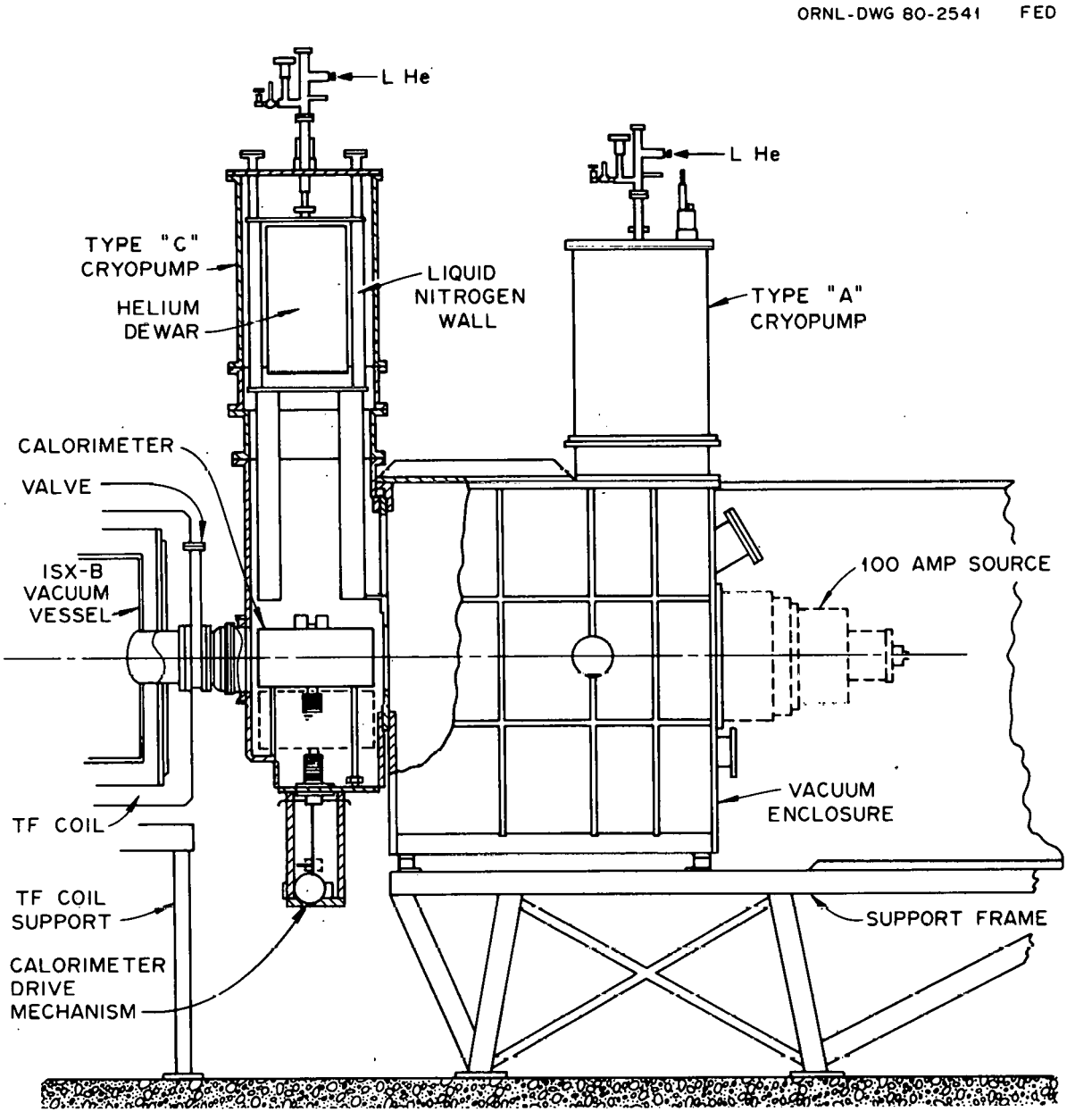

Fig. 21. Neutral Beam Upgrade.

development program. The upgraded beamlines are being operated with the old 22-cm sources until the more powerful sources are ready.

As of June 15, 1980, both 30-cm sources were operational on the beamlines and injection experiments had been done with neutral power up to 1.7-1.8 MW. One source had been conditioned to 1.5 MW H^0 (2.0 MW D^0) by the Plasma Technology Section, and the other (the first installed on ISX) was conditioned on the ISX beamline. The new power monitoring system was working well on both beamlines.

THIS PAGE

WAS INTENTIONALLY

LEFT BLANK

REFERENCES

1. W. L. Stirling et al., "Properties of an Intense 40-kV Neutral Beam Injector," Rev. Sci. Instrum. 50(5), 523-7 (1979).

2. G. G. Kelley et al., "Neutral Beam Injection Heating of Toroidal Plasmas for Fusion Research," Nucl. Fusion 13, 169-176 (1972).

3. J. Kim et al., "ISX-B Neutral Beam Injector Experiment on a Prototype Beam Line," Oak Ridge National Laboratory Report ORNL/TM-6896, Oak Ridge, Tennessee (September 1979).

4. W. L. Stirling, C. C. Tsai, and P. M. Ryan, "15-cm DuoPIGatron Ion Source," Rev. Sci. Instrum. 48(5), 533-6 (1977).

5. C. C. Tsai, W. L. Stirling, and P. M. Ryan, "Plasma Studies on a DuoPIGatron Ion Source," Rev. Sci. Instrum. 48(6), 651-5 (1977).

6. J. Kim and H. H. Haselton, "Analysis of Particle Species Evolution in Neutral Beam Injection Lines," J. Appl. Phys. 50(6), 3802-7 (1979).

7. W. K. Dagenhart et al., "Drift Tube Beam Blocking Experiments Performed on the ORNL/PLT Neutral Beam Line at the ORNL Medium Test Facility," Oak Ridge National Laboratory Report ORNL/TM-6374, Oak Ridge, Tennessee (July 1978).

8. P. H. Edmonds and J. W. Pearce, "A Calorimeter for Pulsed Energy Sources," Proc. 8th Symp. on Engineering Problems of Fusion Research, to be published.

9. P. H. Edmonds, B. Sherrill, and J. W. Pearce, "Computer-Controlled Data Acquisition System for the ISX-B Neutral Injection System," Oak Ridge National Laboratory Report ORNL/TM-7282, Oak Ridge, Tennessee (March 1980).

THIS PAGE

WAS INTENTIONALLY

LEFT BLANK

ORNL/TM-7452
Dist. Category UC-20f

INTERNAL DISTRIBUTION

1-5. S. C. Bates
6-10. C. E. Bush
11-15. P. H. Edmonds
16. W. L. Gardner
17. G. E. Gorker
18. H. H. Haselton
19. D. P. Hutchinson
20. P. W. King
21. J. F. Lyon
22. L. A. Massengill
23. M. M. Menon
24. J. T. Mihalczo
25. M. Murakami
26. G. H. Neilson
27. D. R. Overbey
28. J. W. Pearce
29. J. A. Rome
30. S. D. Scott
31. J. Sheffield
32. W. L. Stirling
33. C. C. Tsai
34. C. E. Thomas
35. J. H. Whealton
36-37. Laboratory Records Department
38. Laboratory Records, ORNL-RC
39. Document Reference Section
40-41. Central Research Library
42. Fusion Energy Division Library
43. Fusion Energy Division Reports Office
44. ORNL Patent Office

EXTERNAL DISTRIBUTION

45. D. J. Anthony, Energy Systems and Technology Division, General Electric Company, 1 River Road, Bldg. 23, Room 290, Schenectady, NY 12345
46. J. Ayers, ORTEC, Inc., Midland Road, Oak Ridge, TN 37830
47. P. R. Bell, 132 Westlook Circle, Oak Ridge, TN 37830
48. N. A. Davies, Tokamak Branch, Office of Fusion Energy, Department of Energy, Washington, DC 20545
49. S. O. Dean, Office of Confinement Systems, Office of Fusion Energy, Department of Energy, Washington, DC 20545
50. H. K. Forsen, Exxon Nuclear Company, Inc., 777 106th Ave., NE, Bellevue, WA 98009
51. H. P. Furth, Princeton Plasma Physics Laboratory, P.O. Box 451, Princeton, NJ 08540
52. D. A. Gedcke, ORTEC, Inc., Midland Road, Oak Ridge, TN 37830
53. R. W. Gould, California Institute of Technology, Mail Stop 116-81, Pasadena, CA 91125
54. C. C. Harris, Department of Nuclear Medicine, Duke University, Durham, NC 27706
55. E. G. Harris, Department of Physics, University of Tennessee, Knoxville, TN 37916
56. K. W. Hill, Princeton Plasma Physics Laboratory, P.O. Box 451, Princeton, NJ 08540
57. R. L. Hirsch, Exxon Research and Engineering Co., P.O. Box 101, Florham Park, NJ 07932
58. T. Hsu, Office of Confinement Systems, Office of Fusion Energy, Department of Energy, Washington, DC 20545

59. G. L. Jahns, General Atomic Co., P.O. Box 81608, San Diego, CA 92138
60. J. Kim, General Atomic Co., P.O. Box 81608, San Diego, CA 92138
61. D. H. McNeill, Princeton Plasma Physics Laboratory, P.O. Box 451, Princeton, NJ 08540
62. A. P. Navarro, Division de Fusion, Junta de Energia Nuclear, Avda. Complutense, Madrid (3), Spain
63. J. Rice, Francis Bitter National Magnet Laboratory, Massachusetts Institute of Technology, Cambridge, MA 02139
64. R. H. Rohrer, Department of Physics, Emory University, Atlanta, GA 30322
65. M. M. Satterfield, The Nucleus, 461 Laboratory Road, Oak Ridge, 37830
66. R. J. Taylor, Center for Plasma Physics and Fusion Engineering, University of California, Los Angeles, CA 90024
67. S. von Goeler, Princeton Plasma Physics Laboratory, P.O. Box 451, Princeton, NJ 08540
68. Office of Assistant Manager for Energy Research and Development, DOE-ORO, Oak Ridge, TN 37830
69-260. Given distribution as shown in TID-4500, Magnetic Fusion Energy (Distribution Category UC-20 f, Experimental Plasma Physics)